CrossMark

INVITED REVIEW

This section of Journal of Materials Research is reserved for papers that are reviews of literature in a given area.

Graphene based biosensors for healthcare

Trupti Terse-Thakoor[a)]
Department of Bioengineering, University of California, Riverside, California 92521, USA

Sushmee Badhulika
Department of Electrical Engineering, Indian Institute of Technology, 502285 Hyderabad, India

Ashok Mulchandani[b)]
Department of Chemical & Environmental Engineering, University of California, Riverside, California 92521, USA

(Received 17 January 2017; accepted 4 April 2017)

Graphene due to its unique physicochemical properties mainly its large surface to volume ratio, excellent thermal and electrical conductivity, biocompatibility, as well as broad electrochemical potential, has received considerable attention for biosensing applications. In this review paper, we provide a comprehensive overview of the recent advances in the field of electrochemical biosensors developed using the graphene nanomaterial including graphene oxide, reduced graphene oxide, CVD graphene, and various graphene based nanostructures including nanomesh, nanowalls, etc. in healthcare related applications. The review focusses on material synthesis, device fabrication, and biofunctionalization of graphene electrodes in biosensing such as those based on electrochemical impedance, amperometry/voltammetry, potentiometry, conductometry, and field effect transistor. Additionally, several ingenious biosensing strategies of graphene biosensor in clinical diagnosis for detection of proteins (disease biomarkers), nucleic acids (mutation analysis in genetic diseases), small molecules (disease metabolites like glucose, lactic acid etc.), and pathogens (bacterial and viral infections) have also been discussed.

I. INTRODUCTION

Biosensor technology has truly revolutionized the quality of human life by providing selective, sensitive, and rapid (point-of-care) detection tools for disease diagnosis and monitoring. Whether it is detection of disease specific, small molecule metabolites like glucose, protein biomarkers, DNA or pathogenic microorganisms, biosensors are being increasingly used in developing advanced detection techniques in healthcare and medicine.

In general, a biosensor can be broadly defined as a device which can detect presence of chemical or biological molecules like enzymes or proteins or nucleic acid, microorganisms, using specific biorecognition elements like receptors, antibodies, enzymes, substrate etc. The information about specific binding of analyte to biorecognition element is converted into a measurable output as a signal using the transducer. Depending upon the type of transducer used, biosensors can be categorized as electrochemical, optical, thermal, piezoelectric etc. To limit the scope of this review, we will be specifically focusing on the electrical/electrochemical biosensors used in healthcare. In electrical/electrochemical biosensors, transducer element converts the biological event such as affinity capture or biocatalytical conversion corresponding to concentration of analyte into an electrical signal such as current or voltage, based on either amperometric, potentiometric, conductometric, or field effect transistor principles. Figure 1 shows the basic design of electrochemical/electrical biosensor.

With the discovery of carbon nanomaterials and advancement in nanofabrication methods and tools, carbon nanotubes (CNTs) and graphene have been extensively explored as transducer elements in the development of biosensor devices. Graphene, in particular has become a popular choice in the development of electrochemical biosensor devices due to its excellent electrical, chemical, and material properties which include large surface area, charge carrier concentrations, and exceptional electron mobility with ballistic electron transport. Moreover the reactivity of graphene edges and functional groups introduced in the basal plane due to its synthesis procedure for e.g., oxygen containing groups introduced during graphene oxide synthesis by Hummer's method are crucial in electrochemical reactions and its functionalization with biorecognition elements.

In this paper, we specifically review electrical/electrochemical biosensors developed using graphene oxide, reduced graphene oxide, CVD graphene, and various

Contributing Editor: Venkatesan Renugopalakrishnan
Address all correspondence to these authors.
[a)]e-mail: tters001@ucr.edu
[b)]e-mail: adani@engr.ucr.edu
DOI: 10.1557/jmr.2017.175

 © Materials Research Society 2017

https://doi.org/10.1557/jmr.2017.175 Published online by Cambridge University Press

graphene nanostructures including nanoribbons and nanowalls and their application in healthcare for clinical diagnosis. Various aspects of graphene based biosensors development such as material synthesis, properties, electrode fabrication, and biofunctionlization have been comprehensively discussed. Finally we have focused on graphene biosensor applications in detection of DNA, metabolites/small molecules, protein biomarkers and pathogens in the form of *in vitro* POC devices as well as wearable and implantable biosensors.

II. MATERIAL SYNTHESIS AND PROPERTIES

A. Graphene

Graphene is a sp^2 hybridized carbon, arranged perfectly in a honeycomb structure to form a 2D monolayer of graphitic structure analogous to a polycyclic aromatic hydrocarbon of quasi infinite size.[1] Though theoretically graphene was known many decades ago, Geim and Novoselov first isolated the graphene by repeatedly peeling the bulk graphite using simple scotch tape in 2004.[2] This mechanical exfoliation method resulted in pristine monolayer to few-layer graphene material [Fig. 2(a)]. The exceptionally superior properties of graphene have been demonstrated using this mechanically exfoliated graphene.[2] Though this method resulted in superior quality graphene, it has shortcomings such as large scale synthesis, poor transfer methods which limits its use in fabricating devices at a commercial scale. Another class of method, used in 19th century which is also based on the exfoliation of graphite using strong acids and oxidizers, is named as chemical exfoliation. Brodie, Staudenmaier, and Hummer methods are the examples of chemical exfoliation methods.[3] Hummer's method is one of the most commonly used methods. This method does not produce pristine graphene, rather results in graphene oxide (GO) sheets [Fig. 2(b)]. These oxygenated functional groups generate defects in sp^2 plane of graphene, rendering it electronically less conductive. But the conductivity can be restored to greater extent by subsequent reduction methods (thermal, chemical, or electrochemical) to produce reduced graphene oxide (RGO). Low cost, ease of processing, aqueous solubility/dispersibility, the presence of reactive edges due to abundance of oxygen functional groups makes GO a popular material in electrochemical biosensors development.

Other synthesis methods reported include, epitaxial growth of high-crystalline graphene using single crystalline silicon carbide (SiC) substrate (4H or 6H-SiC).[4,5] In this process, Si undergoes thermal desorption in ultra-high vacuum with subsequent rearrangement of carbon atoms to produce mono[6] to multilayer graphene.[5,7] The

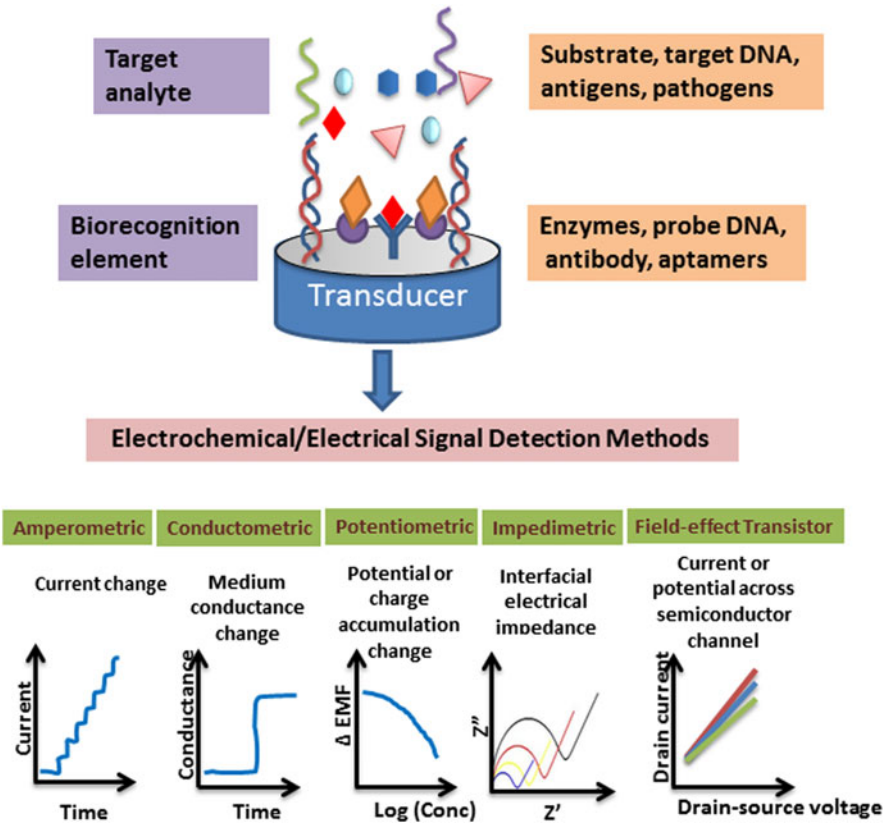


FIG. 1. Schematic of electrochemical/electrical biosensor design.

https://doi.org/10.1557/jmr.2017.175 Published online by Cambridge University Press

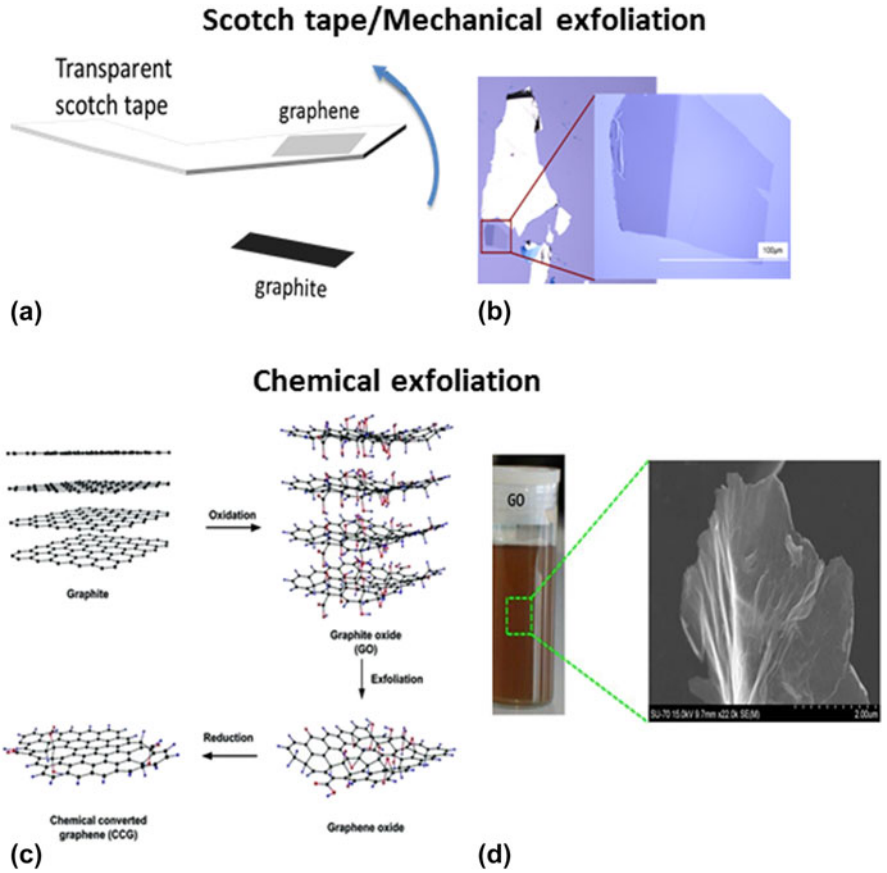


FIG. 2. Mechanically exfoliated graphene (a) schematic of scotch tape method (b) optical image of monolayer graphene on SiO_2/Si produced by scotch tape. Adapted from Ref. 9 chemically exfoliated graphene (c) Schematic of Hummer's method of exfoliating graphene layers from graphite. Adapted from Ref. 10. Reprinted with permission from John Wiley and Sons (2011) (d) optical and SEM image of GO. Adapted from Ref. 11.

advantage of epitaxial graphene (EG) is that it can be grown on large area semi-insulating SiC wafer without need of any graphene layer transfer process.[8] This makes it amenable for device fabrication for semiconductor based miniaturized electrical biosensors. Obtaining uniform thickness with large domains, cost of SiC and transfer of graphene on to another substrate due to its interfacial bonding to SiC, possess some challenges in their application. Epitaxial growth of graphene using hydrocarbon decomposition on various other single crystal metal surfaces like Pt, Ru, TiC, Cu has been reported in the past.[12]

Chemical vapor deposition (CVD) method is currently being extensively studied in synthesis of wafer-scale, large area graphene for large scale device fabrication. Efforts are ongoing in the development of CVD growth protocol with controlled number of graphene layers with desired grain morphology and dimensions. Most commonly, in a typical CVD synthesis of graphene, a metallic planar foil (e.g., Cu or Ni) or 3D foam (e.g., Ni foam) is used as catalytic substrate for the growth. Carrier gas (argon), reducing gas (hydrogen), and carbon precursor gas (mostly methane) are passed at a desired flow rates ratio through a tube loaded with a growth substrate in a temperature controlled furnace. Figures 3(a) and 3(b), respectively, show schematics of typical CVD set up and growth mechanism of graphene at Cu and Ni surfaces. At pyrolytic temperature (about 1000 °C) of carbon precursor gas, single layer graphene (SLG) can be grown on copper surface [Fig. 3(c)] based on a self-limiting process whereas few layer (FLG) to multilayer graphene (MLG) can be grown on the Ni substrate [Fig. 3(d)] due to higher solubility of C in Ni. Use of Ni foam as substrate in CVD growth process has been reported to synthesize the 3D graphene foam [Fig. 3(e)].

Though graphene can be grown at large scale using CVD process, its typical transfer processes includes polymer coating, etching of metallic substrate using iron chloride solution which can introduce ion or polymer impurities, affecting its electrical characteristics. With ongoing development in improving transfer/processing technologies,[18–20] CVD graphene holds great promise for electronics and sensor device fabrication.

As mentioned earlier, the defect rich, water soluble/dispersible GO based material is a popular material in electrochemical biosensing as reactive defects/edges are

https://doi.org/10.1557/jmr.2017.175 Published online by Cambridge University Press

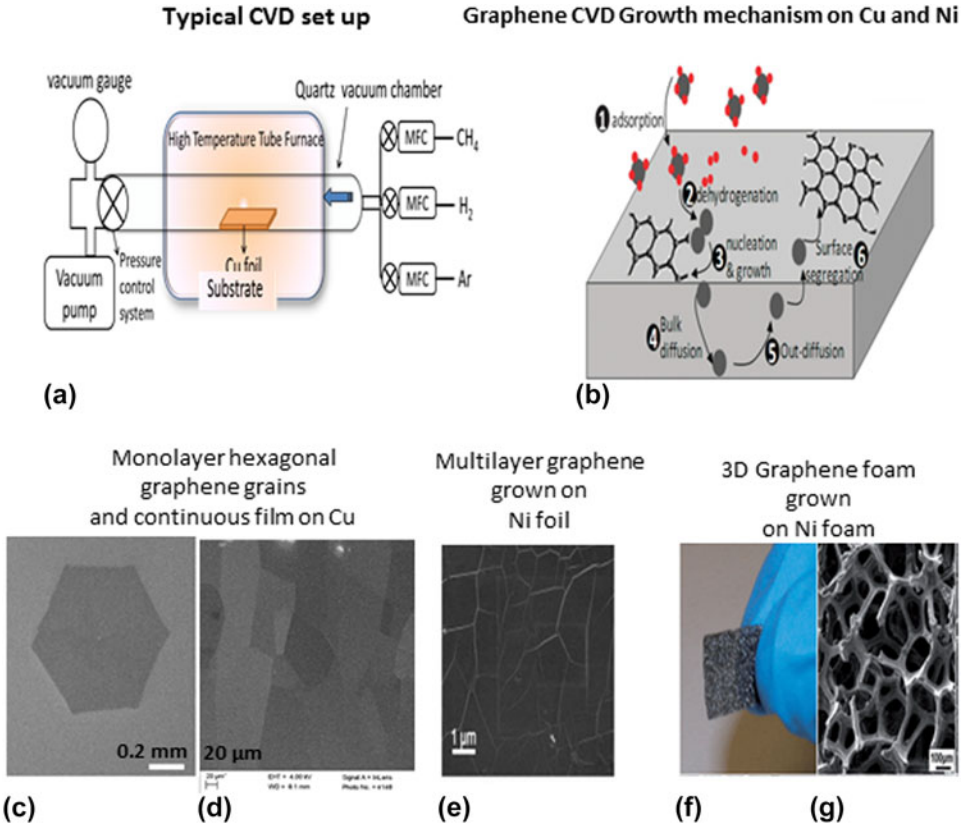


FIG. 3. (a) Schematic of typical CVD set up. Adapted from Ref. 13. (b) Sketch of graphene growth by both direct chemisorptions/deposition on Cu (step 1 to 3) and precipitation/segregation on Ni (step 1, 2, 4, 5, and 6). Adapted from Ref. 14. SEM image of graphene grown on Cu foil (c) monolayer graphene grains. Reprinted by permission from Macmillan Publishers Ltd: [Nature communications] Ref. 15, copyright (2013) (d) continuous graphene film. (e) Multilayer graphene film grown on Ni foil and transferred on SiO_2/Si on Ni foam. Adapted from Ref. 16. Reprinted with permission from Elsevier (2012) (f) optical image of 3D graphene foam. (g) SEM image of graphene foam. Adapted from Ref. 17 with permission of The Royal Society of Chemistry (2014).

crucial for heterogeneous electron transfer (HET) at the electrode surface for redox reactions and for biofunctionlization. In addition, solution processibility of GO based materials is advantageous in incorporating electroactive molecules for electrochemical sensing. But at the same time GO as well as RGO lacks the ideal electrical properties of pristine graphene. Large area CVD graphene film is almost defect free material with intact sp^2 structure shows poor HET therefore more widely used in FET based biosensors than electrochemical based. Raman spectra and cyclic voltammetry measurements of these materials characterize the structural defects and corresponding electrochemical activity.[3,21] To further enhance their performance in biosensing advanced graphene nanoarchitectures and graphene based hybrids/composites have been synthesized. To limit the scope of this article we haven't discussed graphene hybrids in this review as our group have already comprehensively reviewed the synthesis and applications of graphene hybrids.[22]

B. Advanced graphene nanostructures

Apart from planar graphene structures, various advanced graphene nanostructures have been synthesized to enhance their electrocatalytic activity, surface area, and conductivity for use in electrochemical biosensors. These nanostructures with improved properties over planar graphene, are quite newer to the field, and hence have very few literature reports of biosensor applications.

1. Graphene nanoribbons

Graphene nanoribbons (GNRs), which are thin strips of graphene of width 100 nm or less, can be simply visualized as single or multiwall CNTs cut along its parallel axis and unfolded to form planar structure of width corresponding to diameter of the CNTs. GNRs can be synthesized by (i) bottom up organic synthetic approach,[23] (ii) e-beam/ion beam lithographic methods to pattern the exfoliated graphene[24,25] followed by oxygen plasma etching and (iii) unzipping CNTs through chemical oxidation[26] or Ar plasma etching.[27] GNRs produced through chemical oxidation methods are referred as graphene oxide nanoribbons (GONRs) [Figs. 4(a) and 4(b)]. Similar to GO, these GONRs are further reduced to restore its electronic conductivity depending on the extent of oxidation. GNRs produced through lithographic methods

https://doi.org/10.1557/jmr.2017.175 Published online by Cambridge University Press

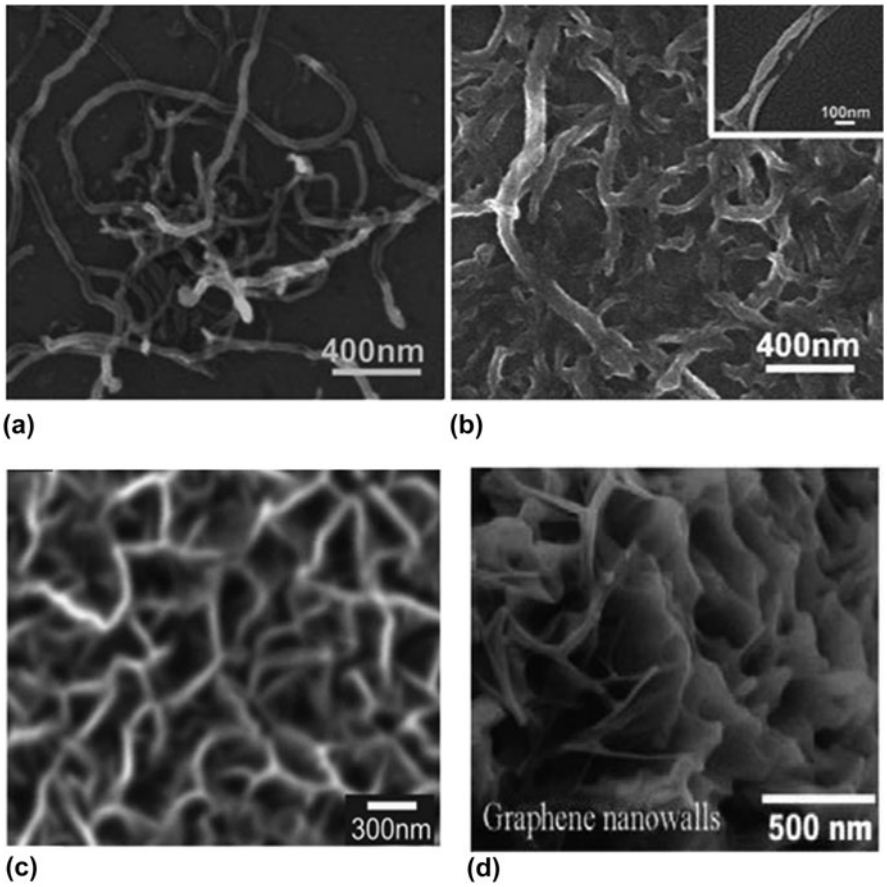


FIG. 4. SEM images (a) multiwalled carbon nanotubes (MWCNTs) before chemical unzipping. Adapted from Ref. 46. (b) Graphene oxide nanoribbons (GONRs) prepared by chemical unzipping of MWCNTs. Adapted from Ref. 46 with permission of The Royal Society of Chemistry (2011). (c) MGNFs grown by microwave plasma enhanced CVD (MPCVD). Adapted from Ref. 35. Reprinted with permission from John Wiley and Sons (2008) and (d) graphene nanowalls synthesized by electrophoretic deposition (EPD). Adapted from Ref. 43. Reprinted with permission from American Chemical Society (2012).

have oxidized/rough edges due to oxygen plasma etching used in their fabrication. Compared to graphene and CNTs, high surface area, edge to basal plane ratio, electroactive defects, and edge chemistry/functional groups of GNRs are advantageous in electrochemical biosensing of analyte.

GNRs are also promising structures as a semiconductor gate/channel material in field effect transistor (FET) based biosensors. The graphene has a zero band gap which limits their sensitivity and limit of detection in FET biosensing[28] In GNRs, the band gap opening is possible by the electronic confinement of the charge carriers in quasi-one dimension due to their narrower widths. Extent of band gap opening largely depends upon the width of the GNRs as well as on presence of defects/edges. Attempts are being made to fabricate GNRs with width down to 10 nm. Still achieving GNRs with smooth edges without any structural disorders or functional groups, induced during their fabrication at high yields is a challenge. The method to produce high quality graphene nanoribbons from CNTs reported by the Dai group at Standford University[29] has been widely used for studying their physical and electronic properties.[30] This method involves first calcination of MWCNTs in air to etch/oxidize the defect sites followed by sonication in 1,2-dichloroethane (DCE) organic solution of poly (*m*-phenylenevinylene-*co*-2,5-dioctoxy-*p*-phenylenevinylene) (PmPV) to unzip them. Other recent methods for high quality GNRs include electrochemical unzipping of MWCNTs.[31]

2. Graphene nanowalls

Graphene nanowalls, which are also called as carbon nanowalls, are mainly multiple graphene sheets assembled or *in situ* grown in vertical or parallel fashion with exposed sharp edges. These graphene nanowalls have a large specific area with higher conductivity and electroactivity, due to its increased edge plane sites, are suitable for development of electrochemical biosensors. The vertical graphene nanowalls structures are grown *in situ* by various PECVD methods using microwave plasma,[32–35] radio frequency (rF),[36] inductively coupled plasma

https://doi.org/10.1557/jmr.2017.175 Published online by Cambridge University Press

(ICP),[37] radical injection,[38] or e-beam excited, conductively coupled,[39] on different substrates such as glass,[40] SiO_2,[34] sapphire, Al_2O_3,[41] NiFe,[32] epitaxial growth on SiC[42] etc., without need of additional catalyst. Whereas parallel graphene nanowalls or layered GO sheets can be synthesized by electrophoretic deposition (EPD) of GO from an electrolyte solution on graphite electrode[43,44] or by simple ultrasonication assisted intercalation methods.[45] Figs. 4(c) and 4(d) shows the SEM images of graphene nanowalls structures grown by microwave plasma enhanced CVD (MPCVD) and EPD method.

III. FABRICATIONS AND BIOFUNCTIONALIZATION OF GRAPHENE ELECTRODES

A. Fabrication of graphene electrodes

Graphene biosensors involving electrochemical measurements using the conventional three-electrode set up employ gold (Au) or glass carbon (GC)[47,48] disk electrodes, indium tin oxide (ITO) coated glass plates,[49] or pyrolytic graphite electrode (PGE)[50] as working electrodes or use disposable electrical printed (DEP) chips with printed carbon electrodes[51] [Fig. 5(a)]. For modification of electrodes with GO, RGO, and GNRs (oxidative unzipped SWCNTs), the materials are first dispersed uniformly in water or ethanol using sonication and the resulting suspension is then drop casted or screen printed on the electrode surface. The solvent is allowed to evaporate and electrode is washed to remove the excess loosely bound material. In another method, negatively charged GO was deposited on the electrode surface through formation of positively charged self-assembled monolayers (SAM) of amine terminated benzenediazonium (ATBD) cation.[52] Fig. 5(b) shows fabrication of graphene electrode using drop casting method as well as through SAM of ATBD on ITO surface.

FET based devices reported in the literature mostly have used CVD grown graphene with few reports of RGO and RGONR based devices.[46,54] CVD graphene grown on Cu or Ni is first coated with

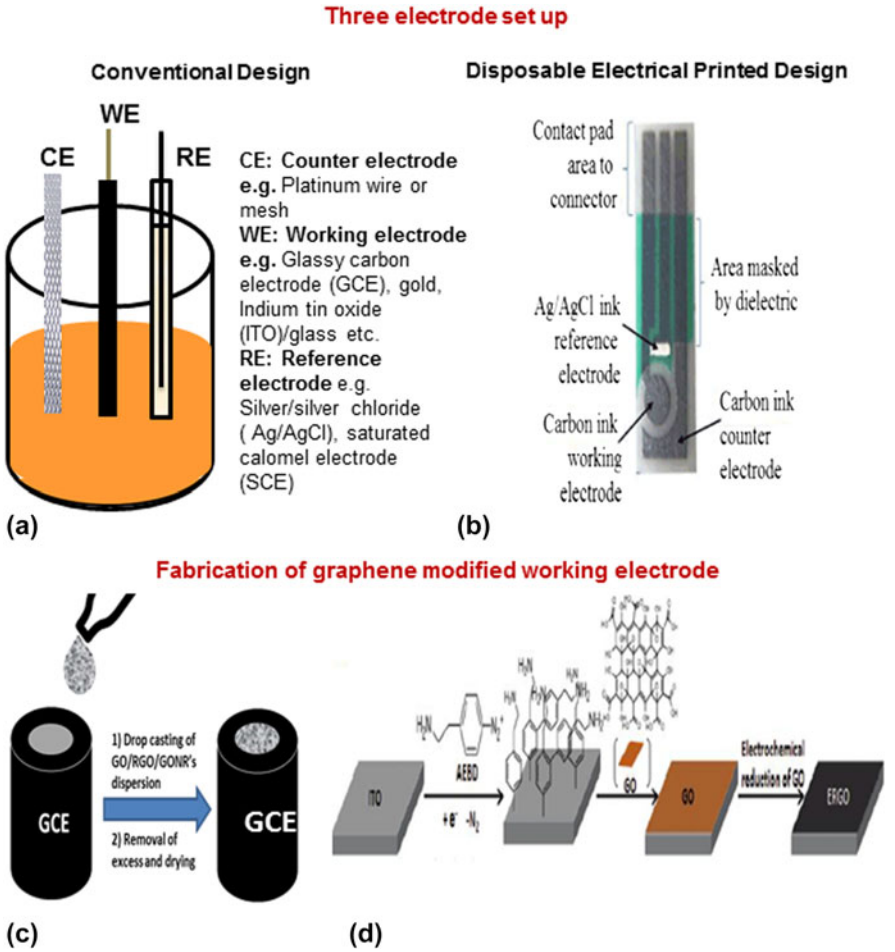


FIG. 5. Three electrode set up for electrochemical measurements using (a) conventional and (b) screen printed disposable designs. Adapted from Ref. 53. Fabrication of graphene working electrodes by (c) simple drop casting and (d) self-assembled monolayer (SAM) of ATBD cation and negatively charged GO. Adapted from Ref. 52. Reprinted with permission from American Chemical Society (2012).

https://doi.org/10.1557/jmr.2017.175 Published online by Cambridge University Press

polymethylmethacrylate (PMMA) polymer for flexibility in transfer process and then its metal substrate is etched in ferric chloride or ferric nitrate solution. PMMA/graphene films floating in water are then transferred by scooping it on suitable substrates to be used as a working electrode and PMMA is removed using solvents such as acetone. For FET device fabrication, the device has either photolithography or EBL patterned source (S) or drain (D) electrodes made of Cr/Au or Ti/Au on graphene/SiO_2/Si substrate[55] or silver paint is used as the S and D electrode on the graphene coated glass slide[56] or SiO_2/Si substrate.[57] Further, for liquid-gated (LG) FET, a liquid chamber is created by insulating electrodes either by using silicon rubber or polydimethylsiloxane (PDMS). In LG-FET, gate voltage is applied through silver wire immersed in the liquid drop placed on the device. Figure 6 shows the design of graphene FET based biosensor including back gate and liquid gated FETs.

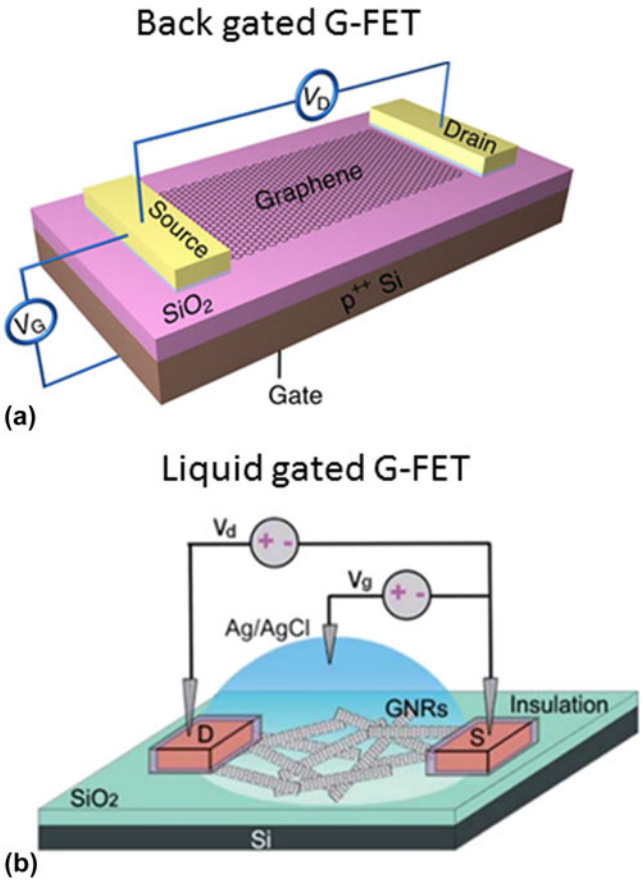


FIG. 6. FET-based graphene biosensor design: back gated G-FET (a) device structure and the circuit diagram corresponding to measurement of I_{SD} (V_G) Adapted from Ref. 55. Reprinted by permission from Macmillan Publishers Ltd: [Nature communications], copyright (2013). (b) Liquid gated G-FET using RGONR thin film as a conducting channel with Ag/AgCl electrode immersed in phosphate buffer saline for applying the gate voltage and electrodes are insulated using silicon rubber. Adapted from Ref. 46 with permission of The Royal Society of Chemistry (2011).

Advanced structures like graphene nanowalls are grown directly *in situ* by PECVD or EPD on the desired electrode substrates as mentioned above. Epitaxial graphene also do not need any transfer process as they are grown directly on the SiC substrate.

B. Biofunctionalization of graphene electrodes

Functionalization of graphene electrode with biorecognition elements such as proteins, aptamer, or DNA can be done using simple physical adsorption through hydrophobic interactions, using electrostatic or covalent binding through oxygenated functional groups of GO or RGO or noncovalent binding through chemical bi-linker molecules.

For covalent functionalization of GO based electrode, widely used approach is to link its carboxylic groups to amine groups of biorecognition elements through amide bond formation, using crosslinker chemistry. For example, probe DNA with 5′-NH_2 group was immobilized on GO/GCE electrode by covalent linkage to carboxylic groups on GO using EDC [1-ethyl 3-(3-dimethylaminopropyl)carbodiimide·HCl] crosslinker and *N*-hydroxysuccinimide (NHS) chemistry.[58]

Biomolecules functionalization through π–π interaction using sp^2 basal plane of GO, RGO, or CVD graphene or hydrophobic interactions by bi-linker molecules is a common approach used in graphene based devices. In this method one end of the bi-linker molecule such as 3,4,9,10-perylene tetracarboxylic acid (PTCA), 1-pyrenebutanoic acid succinimide ester (pyrene-NHS) and poly(BMA-r-PEGMA-r-*N*-acryloxysuccinimide), binds to the graphene surface via π–π bond or hydrophobic interaction while the other end reacts with the –NH_2 group of the biomolecule.[47,59,60] Fig. 7 shows the NH_2-ssDNA functionalization of graphene through PTCA linker and EDC/NHS chemistry.

IV. GRAPHENE ELECTRICAL/ELECTROCHEMICAL BIOSENSOR APPLICATIONS

A. DNA biosensing

DNA biosensing in healthcare is crucial in screening and diagnosis of human genetic diseases by detecting single nucleotide polymorphisms (SNPs), human pathogenic diseases to identify the pathogens based on their specific DNA sequences,[61–64] DNA damage caused by chemical agents e.g., acrylamide etc., anticancer drugs, nucleases, ionizing radiations, and studying the interaction.[50,65,66] Development of DNA diagnostics from biosensor to gene chips to miniaturized 'Lab-on-Chip' device for rapid, simple, massively parallel yet accurate and highly sensitive analysis of DNA is intense.[64,67]

Graphene has been successfully used as a platform in the development of DNA biosensor due to difference in

https://doi.org/10.1557/jmr.2017.175 Published online by Cambridge University Press

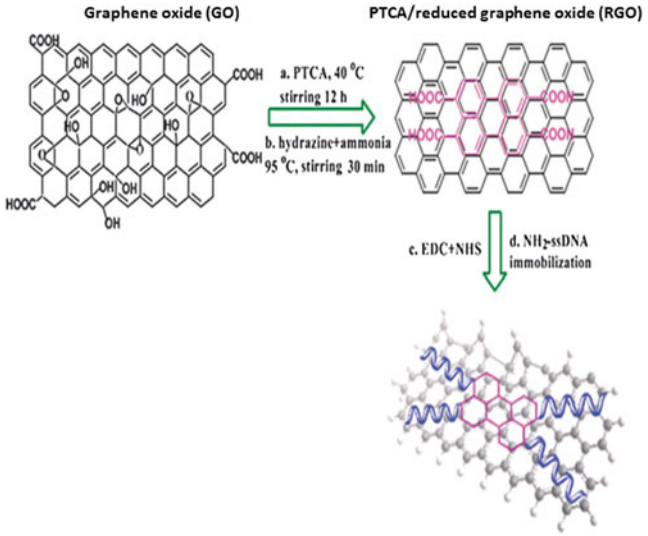


FIG. 7. Schematic representation of noncovalent functionalization of graphene using 3,4,9,10-perylene tetracarboxylic acid (PTCA) linker to introduce carboxylic groups and subsequent functionalization with probe ssDNA. Adapted from Ref. 47 with permission of The Royal Society of Chemistry (2010).

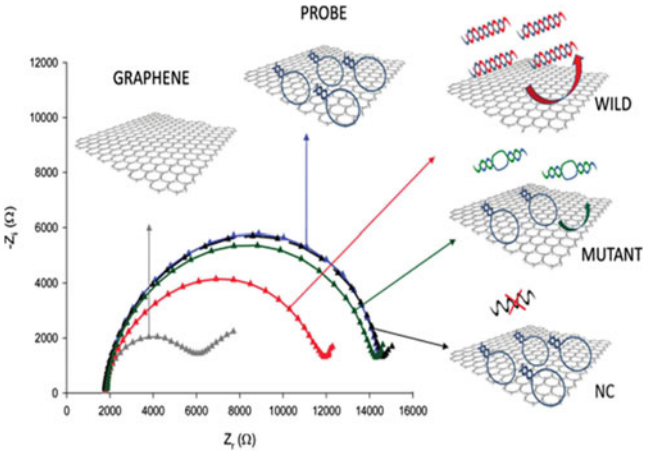


FIG. 8. Schematic of the protocol and Nyquist plots for "signal-off" impedimetric DNA biosensing of the graphene surface (gray), hairpin pDNA (blue), complementary target (red), 1-mismatch target (green), and negative control with a noncomplementary sequence (black). All measurements were performed in PBS buffer solution containing $K_3[Fe(CN)_6]/K_4[Fe(CN)_6]$. Adapted from Ref. 69. Reprinted with permission from American Chemical Society (2011).

the binding affinity of ssDNA and dsDNA to graphene. It has been reported that ssDNA binds strongly to graphene than dsDNA due to its structural flexibility and maximally exposed nucleobases for interaction with the graphene plane. These nucleobases mainly bind through their aromatic groups to sp^2 basal plane of graphene by π–π interaction. Also, they are shown to bind to graphene in different morphological shapes (spherical particles or elongated networks) depending upon the magnitude of the interaction energies between nucleobases and between graphene and nucleobases.[68]

Graphene based electrochemical DNA sensing is based on two major principles: (i) detection of hybridization event between the probe DNA (pDNA) and target DNA (tDNA) (ii) direct detection of bases of DNA by monitoring their oxidation.

Electrochemical impedance spectroscopy (EIS) is a popular method in hybridization based DNA biosensing due to its sensitivity in translating the binding events at the electrode and electrolyte interface. "Signal-off" and "signal-on" mode are the two formats for the EIS-based graphene DNA biosensor. In the "signal-off" mode format, ssDNA is immobilized through physical adsorption as a pDNA which upon hybridization with tDNA forms dsDNA duplex and detaches from the graphene surface resulting in the decrease in the impedance signal ("signal-off" mode).[69] Figure 8 shows the schematics of protocol and Nyquist plots for "signal-off" mode impedimetric DNA biosensing. Different chemically modified graphene platforms such as GO, electrochemically RGO (ERGO), and thermally RGO (TRGO), were studied in "signal-off" mode EIS based SNP detection for Alzheimer disease.[51] GO was found to be the best platform amongst them to detect the SNP. In another study, few layer graphene was found to be the most sensitive platform with a LOD of 6.6 pM (linear detection range from 3×10^{-13} to 3×10^{-10} M) when compared to single (LOD 50 nM) and multilayer graphene (LOD 66 μM) for detection of wild type target and was chosen for detecting SNP correlated to the Alzheimer disease.[69] The unique morphology of large area, wavy GO nanowalls providing large specific area with rich conjugated structure for efficient pDNA immobilization and sharp edges for faster electron transfer have resulted in more sensitive "signal-off" based EIS detection of PML/RARA [fusion gene sequence formed from promyelocytic leukemia (PML) and retinoic acid receptor alpha (RARA)] with LOD of 5.20 fM and detection range of 1.0×10^{-7}–1.0×10^{-14} mol/L.[45]

DNA immobilized on GO or RGO by covalent modification through oxygenated groups or by π–π interaction through bifunctional linkers like perylene derivatives anchoring functional groups for DNA attachments results "signal-on" mode EIS detection due to change in the conformation and negative charge accumulation after hybridization with target DNA instead of the detachment in case of "signal-off" EIS. Figure 9 shows the fabrication and "signal-on" impedimetric DNA detection of specific HIV gene sequence.[58] GO was used for immobilization of pDNA through carbodiimide chemistry and then converted the GO electrochemically to ERGO to improve the electron transfer characteristics. The resulting electrode had a LOD of 3×10^{-13} M with linear detection range from 1×10^{-12} to 1×10^{-9} M.

https://doi.org/10.1557/jmr.2017.175 Published online by Cambridge University Press

A disposable amperometric DNA biosensor was reported for the direct detection of tDNA sequence on p53 tumor suppressor (TP53) gene and discriminating between wild and SNP containing sequences using RGO-carboxymethyl cellulose (CMC) nanomaterial.[70] Two different DNA sensing platforms were evaluated by immobilizing biotinylated hairpin capture probe of two different lengths (33 versus 20 nucleotides) on the RGO/CMC modified screen printed carbon electrode (SPCE). Streptavidin-Horseradish peroxidase (Strep-HRP) conjugate was captured on the hybridized duplex and amperometric detection was carried out using 3,3′,5,5′-tetramethylbenzidine (TMB)–H_2O_2 system (Fig. 10). In the case of long pDNA, due to increased distance between Strep-HRP conjugate and electrode, the current response was decreased due to hindrance of enzyme catalyzed electron transfer. On the other hand, in the case of short pDNA amperometric response increased due to decreased hindrance to electron transfer rate.

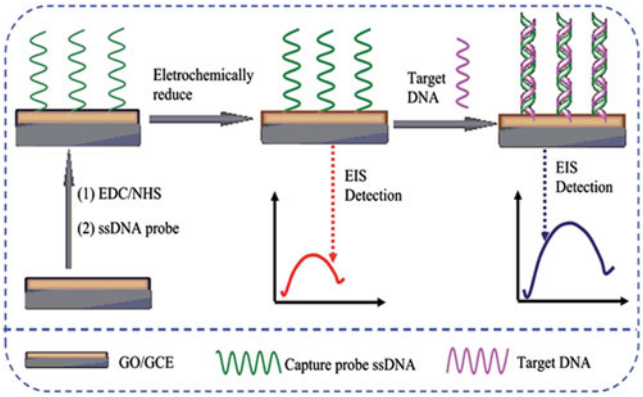


FIG. 9. Schematic diagram of the fabrication of the impedimetric DNA biosensor and the detection of target DNA for "signal-on" mode impedimetric DNA biosensing. Adapted from Ref. 58 with permission of The Royal Society of Chemistry (2015).

Anodized EG with high edge plane defects was found to be a superior platform than pristine EG, boron doped diamond, CNTs, and glassy carbon in simultaneous detection of all four nucleic acids (A, T, G, C) based on their oxidation.[71] All nucleic acids were resolved as individual oxidation peaks using differential pulse voltammetry (DPV) from sample containing free bases, ssDNA and dsDNA.

FET-based devices are of great choice in developing miniaturized chip based POC biosensors for label free

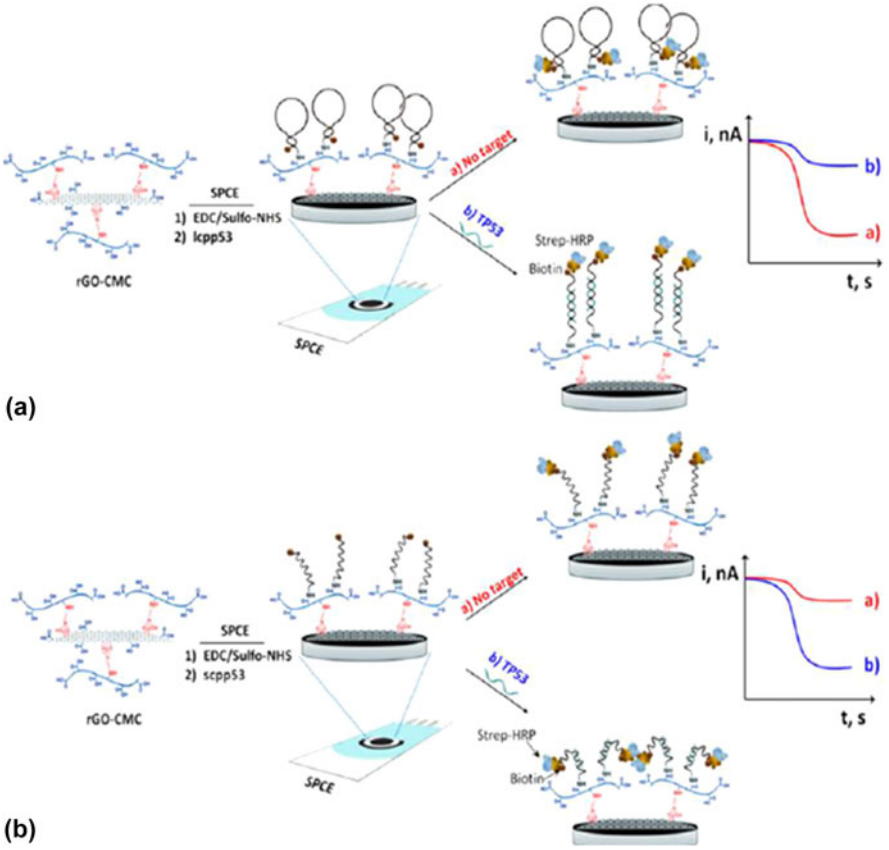


FIG. 10. Schematic illustration of the steps involved in the preparation of the electrochemical DNA biosensor for the detection of the TP53 gene using rGO−CMC hybrid nanomaterial as a scaffold [(a) the long TP53 capture probe (lcpp53) or (b) the short (spp53) TP53 capture probe] and labeling with Strep-HRP (relative sizes of the components are not drawn on a real scale). Adapted from Ref. 70. Reprinted with permission from American Chemical Society (2015).

https://doi.org/10.1557/jmr.2017.175 Published online by Cambridge University Press

detection. CVD graphene has been used to fabricate G-FET (graphene-FET) devices due to ease and reproducibility of device fabrication.[55,57,72] Liquid gated G-FETs have been reported in DNA sensing with single base mismatch specificity.[56,57] Synthetic oligonucleotide (pDNA) was immobilized on the graphene patterned with source and drain electrodes. A drop of buffer containing fully matched tDNA or one-base mismatched ssDNAs was then added. After hybridization reaction, chip is rinsed and fresh drop of buffer was added. Liquid gating was established by using silver wire immersed into the top of the drop. Figure 11(a) shows the schematic of liquid gated G-FET device with DNA sequences used in sensing. Detection was based on the n-doping of graphene with DNA as evident by left shifting of $V_{g,min}$ in transfer curve [drain current (I_d) versus gate voltage (V_g) curve] as shown in Fig. 11(b). Liquid gated G-FET biosensor was developed and Hall effect measurements were performed based on the Van der Pauw method for DNA hybridization detection.[57] It was found that sheet resistance increases and hole carrier mobility of graphene FET devices decreases with increasing concentration of complementary DNA or single base mismatch DNA. Whereas hole carrier concentration increases with added complementary DNA but no significant effect with added one base mismatch DNA.

Table I summarizes the recently reported DNA biosensor using graphene based electrodes.

Modified nucleoside and nucleobases are the selective markers for the wholebody turnover of RNA including tRNA, mRNA, and rRNA. Increased levels of modified nucleoside are found in the urine of the patients with different types of malignancies[81] and AIDS.[82] Therefore detection and quantification of bases of nucleic acids is important in the diagnosis and therapy control of these diseases. Individual and simultaneous detection of adenine and guanine has been reported using carboxylic acid functionalized graphene electrode.[83] The direct electrooxidation of adenine and guanine was studied using cyclic voltammetry and differential pulse voltammetry methods.

B. Protein biomarkers biosensing/ immunosensing

Diseases biomarkers are mainly proteins whose presence or abnormal levels in the body fluids can be used as indicator for diagnosis, progression of a disease or to assess pathophysiological response to a therapeutic treatment. Rapid, selective, and sensitive point of care detection of single or array of biomarkers from body fluids, i.e., blood or urine, on a single biosensor device has opened a promising avenue for early and accurate detection of life threatening diseases like cardiovascular diseases, cancer etc. The promising progress in the biomarkers discovery research through advanced genomic and proteomic methods have facilitated the

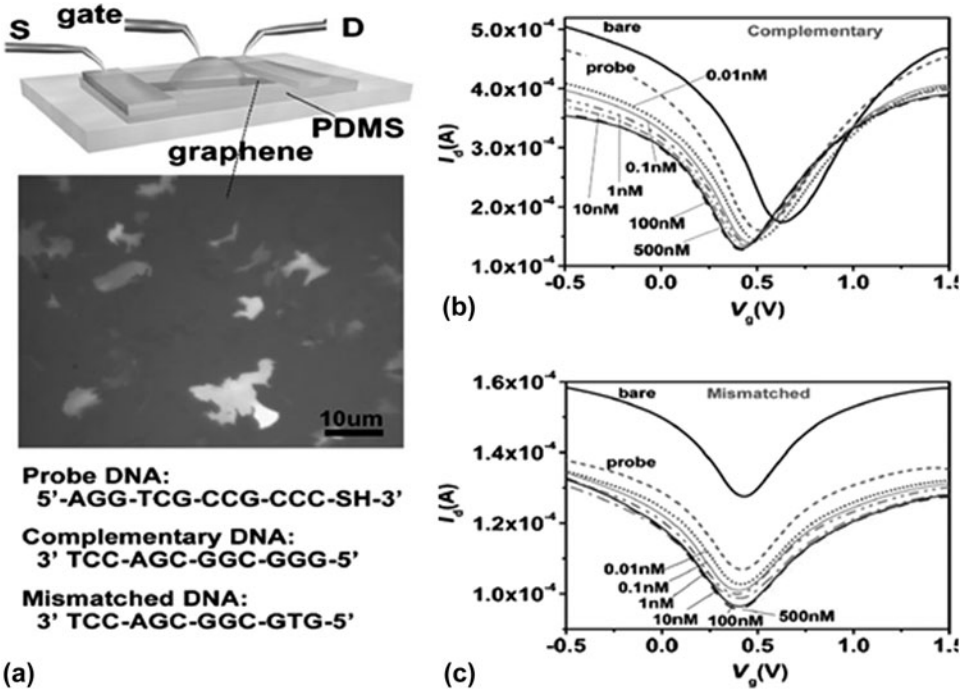


FIG. 11. (a) Schematic illustration of the graphene device operated by liquid gating. Middle is an optical microscopy image of the graphene films. Bottom shows the DNA sequences used in the experiments. Transfer characteristics for the graphene transistors before adding DNA, after immobilization with probe DNA, and after reaction with (b) complementary or (c) one-base mismatched DNA molecules with the concentration ranging from 0.01 to 500 nM. Adapted from Ref. 56. Reprinted with permission from John Wiley and Sons (2010).

https://doi.org/10.1557/jmr.2017.175 Published online by Cambridge University Press

TABLE I. Summary of recently reported DNA biosensors using graphene based electrodes.

Graphene electrode	Target DNA/analyte	Method of detection	LOD	Reference
GCE-APTES-rGO-ssDNA	Methicillin-resistant *Staphylococcus aureus* (MRSA) DNA	Hybridization detection by EIS	1×10^{-13} M	73
GCE/ERGO	HIV-1 gene	Hybridization detection by EIS	3×10^{-13} M	58
PDI/graphene (CRGO)	HIV-1 pol gene sequence	Hybridization detection by EIS	5.5×10^{-13} M	74
CVD graphene/SiO_2/Si	λ DNA	Back gated FET	8×10^{-12} M	55
Anodized EG	Nucleic bases, ssDNA and dsDNA	Direct oxidation of nucleic bases by voltammetric measurements by DPV	Not reported	71
RGO/CMC/cDNA/biotin with streptavidin-HRP conjugate (electrochemical indicator) and TMB-H_2O_2 (redox mediator)	TP53 gene	Chronoamperometry	3.4×10^{-9} M (short cDNA) 2.9×10^{-9} M (long cDNA)	70
CVD graphene/SiO_2/Si	Synthetic DNA sequence	Liquid gated FET for hybridization detection	1×10^{-11} M	56
CVD graphene/SiO_2/Si	Synthetic DNA sequence	Liquid gated FET for hybridization detection	1×10^{-12} M	57
PEG/ERGO-ionic liquid/$(HRP/DNA)_n$	Detecting damage in dsDNA by acrylamide and its metabolite	DPV for measuring direct oxidation of guanine	Not reported	50
GC/CRGO/ssDNA	8-Hydroxy-2′-deoxyguanosine (8-OH-dG)	Cyclic voltammetry (CV) for measuring oxidation of 8-OH-dG	8.75×10^{-8} M	75
GC/PAN/ERGO/ssDNA	CaMV35S gene	DPV measurement detecting hybridization	3.2×10^{-14} M	76
ERGO-graphene double-layer electrode	HIV-1 gene	DPV measurement detecting hybridization	1.58×10^{-13} M	77
ITO/CHI-GO/ssDNA	Vi capsular antigen gene region of *S. enteric serovars typhi*	DPV monitoring the oxidation current of Methylene blue redox indicator on hybridization	1×10^{-13} M	49
G-SL, G-FL, G-ML	Wild type Alzheimer gene	Hybridization detection by EIS	5×10^{-8} M (G-SL) 6.6×10^{-12} M (G-FL) 6.6×10^{-7} M (G-ML)	69
GCE/RGO-PTCA	HIV-1 pol gene sequence	Hybridization detection by EIS	5×10^{-13} M	47
GCE/RGO	Amelogenin gene (AMEL)	Hybridization detection by EIS	3.2×10^{-21} M	78
GCE/Ph-NH_2/GO	HIV-1 pol gene sequence	Hybridization detection by EIS	1.1×10^{-13} M	48
Spongy graphene electrodes	Detection of leukemia cells based on guanine oxidation	Oxidation current by DPV	~0.02 cell/mL	79
Nafion-RGO	HIV-1 gene	Hybridization detection by EIS	2.3×10^{-14} M	80

PDI: perylene[54] derivative, *N*,*N*-bis-(1-aminopropyl-3-propylimidazol salt)-3,4,9,10-perylene tetracarboxylic acid diimide, CMC: carboxymethylcellulose, PEG: pyrolytic graphite electrode, HRP: horseradish peroxidase, PAN: polyaniline, CHI: chitosan, Ph-NH_2: phenyl-amino.

development of biosensors including POC devices in clinical diagnosis based on biomarkers detection.

Graphene has been explored mostly in the detection of cancer protein biomarkers such as phosphorylated p53 protein (ovarian cancer),[84,85] carcinoembryonic antigen (CEA) (colorectal cancer),[86] alpha-fetoprotein (AFP) (liver cancer),[86] and cardiac biomarkers such as cardiac troponin I,[87] C-reactive protein,[88] soluble CD40 ligand,[88] etc. Graphene, mainly ERGO has been used as the platform for the antibody/probe immobilization through its functional groups in various sandwich type immunosensors[52] resulting in higher detection sensitivity due to its high electronic conductivity. Apart from using as a platform, graphene has also been used as a nanocarrier in linking enzyme label and signal antibody in signal amplification strategy due to its high loading ratio than gold nanoparticle (AuNP), high surface area, and biocompatibility.[85] Enhanced sensitivity was reported when bioconjugate featuring HRP and $p53^{392}$ (phosphorylated p53 at Ser392) signal antibody linked to functionalized GO was used in sandwich immunoreaction [Fig. 12(c)]. For immunosensing, AuNP modified SPCE is first functionalized with primary antibodies.

Upon sandwich immunoreaction, HRP-$p53^{392}$Ab2-GO conjugate is captured on the electrode. Enzymatic products of HRP in presence of H_2O_2 and thionine are then electrochemically detected. Figures 12(a) and 12(b) shows the schematic of multienzyme labeling amplification strategy and square wave voltammetry measurements at different concentrations of phospho-$p53^{392}$ antigen. This amplification strategy has dynamic range from 0.02 to 2 nM and LOD of 0.01 nM for phosphorylated p53-S392 (phospho-$p53^{392}$).[85]

Recently, CVD grown, 3D monolithic and macroporous graphene foam has been reported for sensitive detection of CEA.[89] Macroporous scaffold with large

https://doi.org/10.1557/jmr.2017.175 Published online by Cambridge University Press

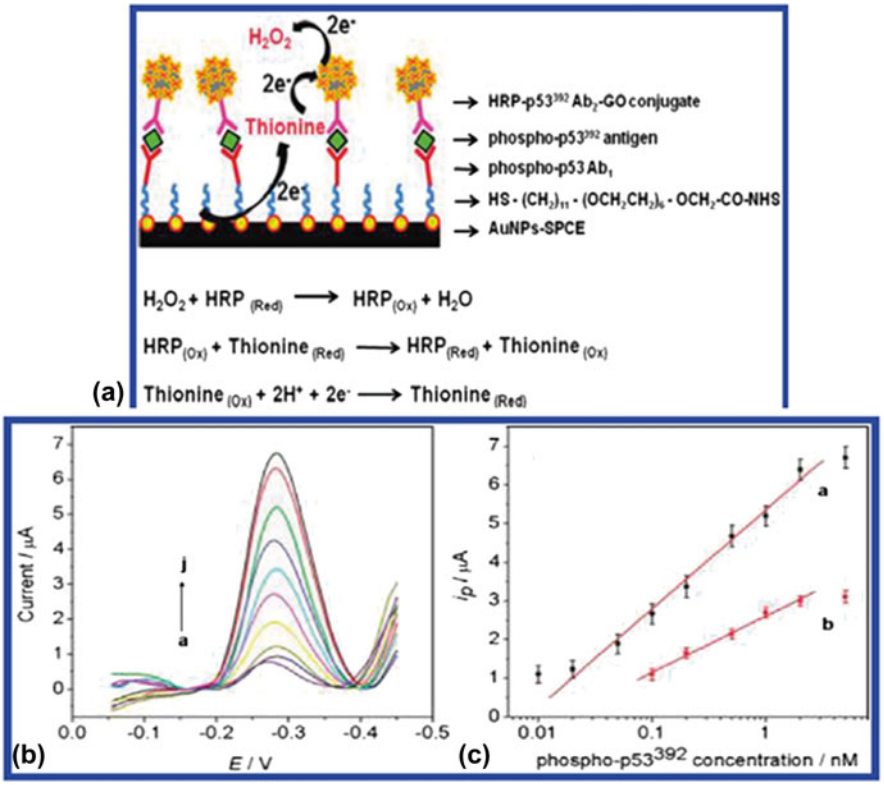


FIG. 12. (a) Schematic illustration of the multienzyme labeling amplification strategy using HRP-p53392Ab2-GO conjugate. (b) Square wave voltammetry curves acquired at HRP-p53392Ab2-GO/phosphop53392/Ab1/NHS/AuNPs-SPCE after incubation with (a) 0–5 ng mL-1 phospho-p53392 antigen in pH 7.4 PBS containing 25 μM thionine and 2 mM H_2O_2. (c) Calibration plots of the (a) proposed HRP-p53392Ab2-GO/phospho-p53392/Ab1/NHS/AuNPs-SPCE and (b) traditional HRP-streptavidin-biotin-p53392Ab2/phospho-p53392/Ab1/NHS/AuNPs-SPCE for detecting phospho-p53392 antigen. Adapted from Ref. 85. Reprinted with permission from American Chemical Society (2011).

electroactive area, superior substrate diffusion along with high conductivity and stability makes 3D graphene foam (3D G foam) superior electrode over conventional planar electrodes. During sensor fabrication, concanvaline A (ConA) lectin was first immobilized on the graphene foam through polydopamine as the linker. HRP labeled anti-CEA antibody was further immobilized on the 3D G foam via biospecific "lectin-sugar protein" interaction between ConA and HRP. Electrochemical detection of CEA was based on the measuring the inhibited current response of redox probe using DPV with increasing concentrations of CEA. Without any complex amplification strategy, the 3D electrode showed good dynamic detection range of 0.1–750 ng/mL with LOD of ~90 pg/mL for CEA detection. In case of CVD grown polycrystalline graphene (PCG), the grain boundaries and carriers scattering from substrate such as SiO_2, largely affects the intrinsic properties of graphene and thus the performance of the sensor. Biosensing performance of LPCVD grown, free standing single crystal graphene (SCG) in multiplex detection of lung cancer biomarkers was studied and compared to the device made with PCG.[90] Fig. 13 shows the SCG sensor fabrication and characterization. The immunoreaction between three tumor biomarkers namely ANXA2, VEGF, and ENO1 in increasing concentration with their corresponding antibodies were detected based on the change in the resistance due to change in the carrier concentration and therefore the mobility of the graphene [Figs. 14(a) and 14(b)]. The SCG biosensor can measure the concentrations as low as 0.1 pg/mL with low frequency of noise over PCG [Fig. 14(c)]. SCG based biosensor showed superior uniformity over PCG based ones. It also exhibited specificity and large linear detection range from 1 pg/mL to 1 μg/mL.

Liquid gated RGO-FET biosensors is reported for label free ultrasensitive detection of prostate cancer biomarker, prostate specific antigen/α1-antichymotrypsin (PSA-ACT) complex.[54] Fig. 15 shows the schematic of fabrication and detection of PSA-ACT complex. The channel conductivity σ (V_g) is obtained at different analyte concentration using PBS solution of pH of 7.4 and 6.2.

The isoelectric point of PSA-ACT is 6.8 so it is negatively and positively charged at pH 7.4 and 6.2, respectively. Using $\Delta V_{g,min}$ as sensing parameter, RGO-FET could detect PSA-ACT complex down to LOD of 100 fg/mL (~1.1 fM). Figure 16 shows the detection characteristic of RGO-FET sensor.

https://doi.org/10.1557/jmr.2017.175 Published online by Cambridge University Press

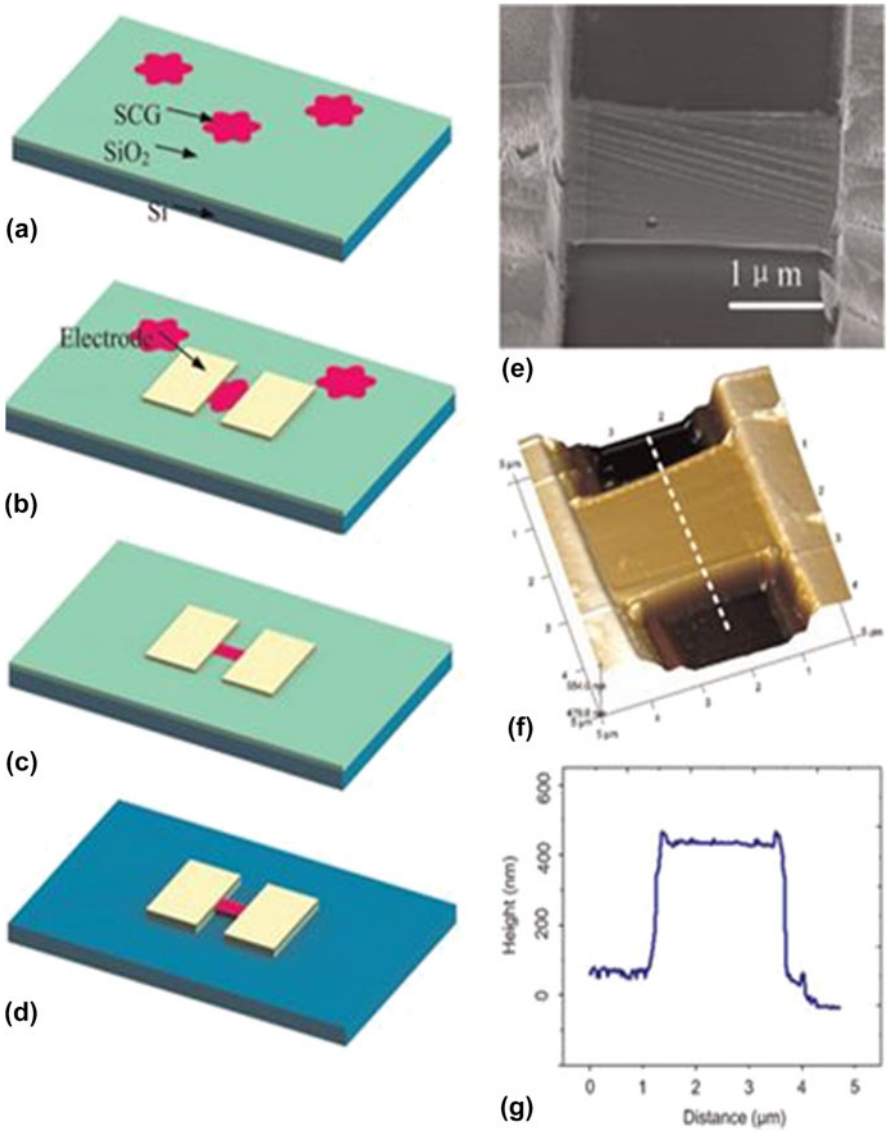


FIG. 13. Suspended, single crystalline graphene (SCG) sensor fabrication. (a–d) process. (a) Transfer SCGs from copper foil onto SiO_2/Si substrate by PMMA assisted process. (b) Choose a SCG and fabricate metal electrodes on it. (c) Etch SCG into rectangular beam shape. (d) Etch SiO_2 beneath to release the suspended SCG beam. (e) SEM image of a suspended SCG beam. (f) AFM topographic image of a SCG beam. (g) The AFM lines scan of SCG beam marked with white dot line confirming SCG is suspended and the distance between the beam and substrate is about 300 nm. Adapted from Ref. 90. Reprinted with permission from Elsevier (2015).

Table II summarizes the reports of graphene based biosensors in protein biomarkers detection and their performance.

C. Metabolites/small molecules biosensing

Low molecular weight compounds such as glucose, dopamine (DA), ascorbic acid (AA), uric acid (UA) which are normally present in the body fluids play important role in the normal functioning of some of the biological processes such as DA in central nervous system or AA in tissue and immune system. They can also be present in the system, being the metabolic products for e.g., UA is the oxidation product in urine metabolism. Their quantitative detection is important in diagnostics as abnormal levels indicates certain metabolic disorders like diabetics,[96] gout/kidney dysfunctioning,[97] neurological disorders like schizophrenia and Parkinson.[98]

Electrochemical glucose biosensors have played a key role in the development of accurate and reliable glucose detection for the diagnosis and management of diabetes. Among them enzyme based amperometric biosensors have been the focus of advanced research and development. Most of the enzyme based glucose biosensors, use glucose oxidase (GOx) enzyme to catalyze the oxidation of glucose

https://doi.org/10.1557/jmr.2017.175 Published online by Cambridge University Press

and indirectly detect glucose by measurement of its oxidation product i.e., hydrogen peroxide (H_2O_2). Direct electrochemical quantification of glucose oxidation can be achieved either using redox mediators or more recently through direct electron transfer (DET) of redox factor of GOx using advanced materials and electrode geometry.

Graphene has been studied for DET and in amperometric glucose biosensing based on the reduction of

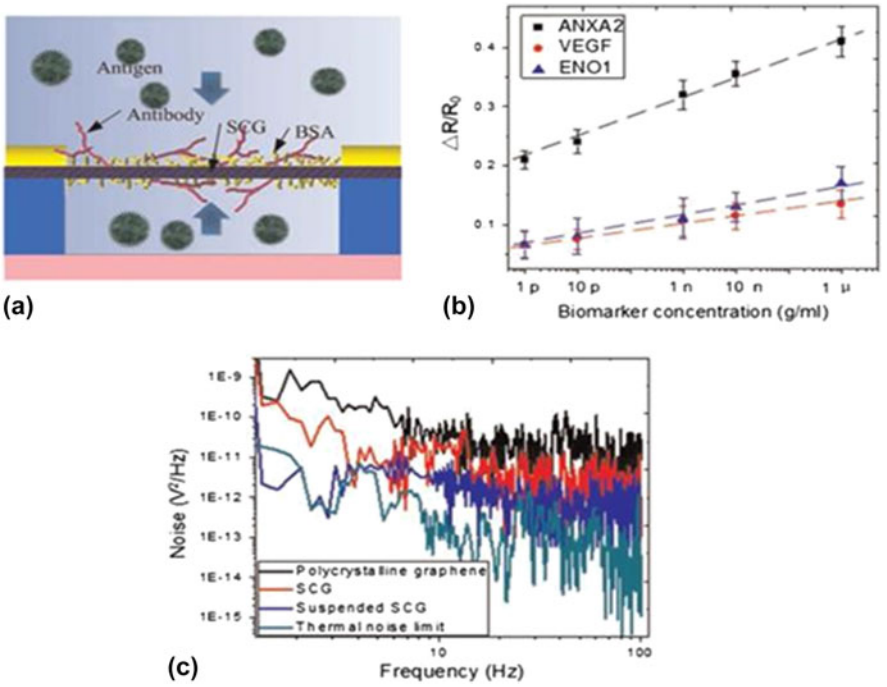


FIG. 14. (a) Schematic illustration of immunoreaction of suspended SCG biosensor. (b) The SCG sensor's response to 3 different types of lung cancer tumor markers. Tumor markers with higher concentration result in larger resistance shift of the sensor. (c) Comparison of low-frequency noise in polycrystalline graphene, nonsuspended SCG and suspended SCG. Suspended SCG has the smallest low-frequency noise. Adapted from Ref. 90. Reprinted with permission from Elsevier (2015).

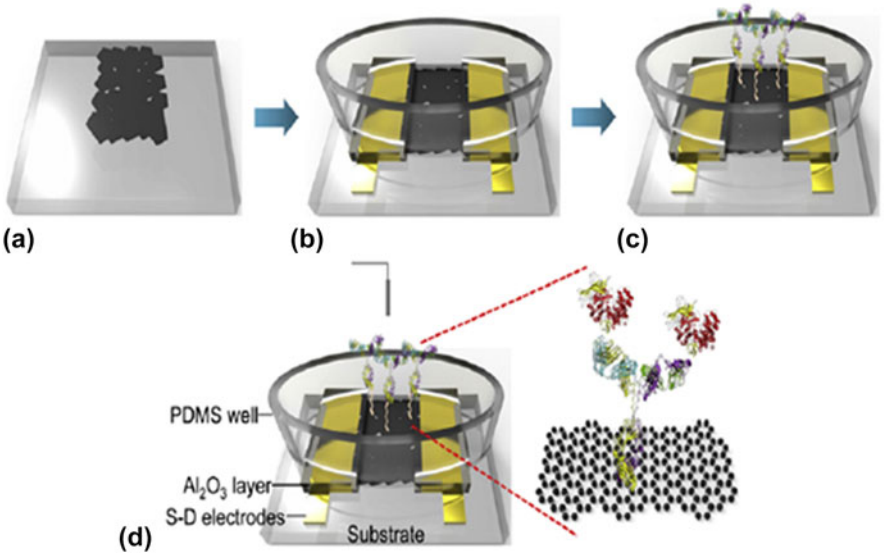


FIG. 15. Schematic of RGO-FET fabrication and detection of PSA-ACT complex. (a) Self-assembly of GO nanosheets on amine SAM substrate and reduction to RGO. (b) Formation of Ti/Au source and drain electrodes, capping of the electrodes by Al_2O_3 and PDMS layers for minimization of leakage currents. (c) Functionalization of RGO channel by linker molecules, immobilization of PSA mAb to the linker molecules on RGO channel, and treatment of ethanolamine (ETA) for nonspecific binding. (d) Illustration of RGO-FET immunosensor with Pt reference electrode in the analyte solution. The immunoreactions between antibody (PSA mAb) and the antigen (PSA-ACT complex) caused changes in the carrier density in the RGO channel due to the doping effects. Adapted from Ref. 54. Reprinted with permission from Elsevier (2013).

https://doi.org/10.1557/jmr.2017.175 Published online by Cambridge University Press

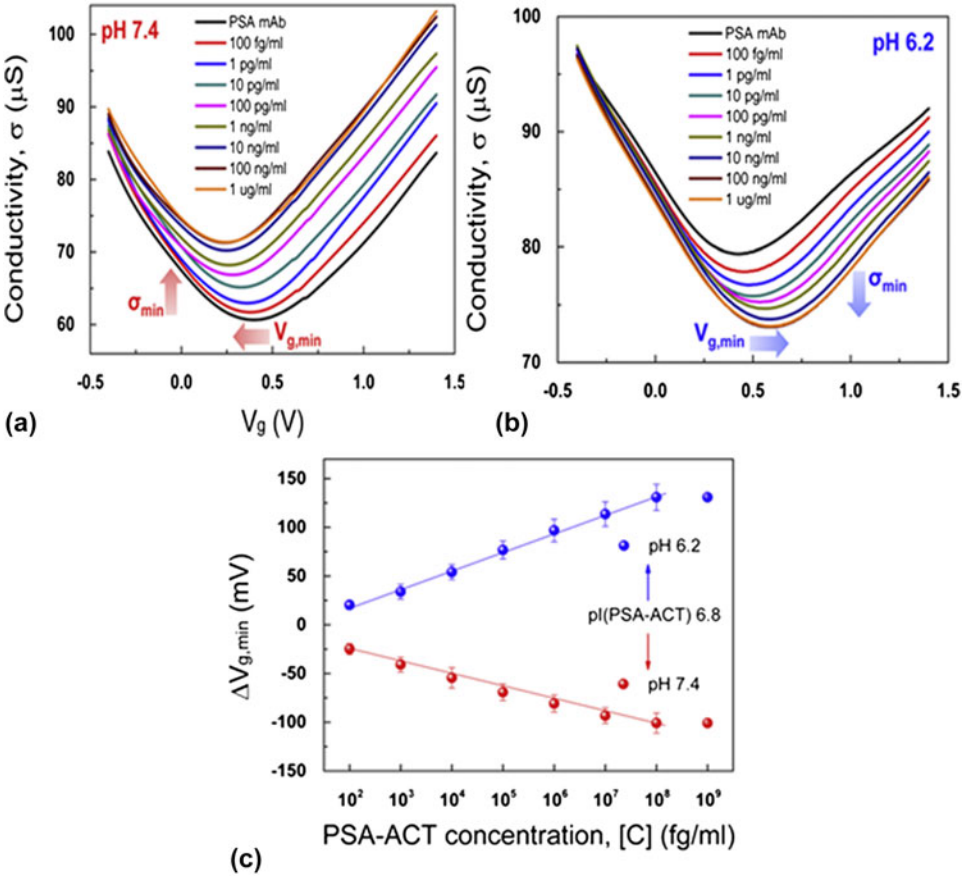


FIG. 16. Detection characteristics of RGO-FET immunosensors. (a–b) σ-V_g plot of RGO-FET at a V_{sd} of 0.6 V with various concentrations of PSA-ACT complex in the analyte solutions at (a) pH 7.4 and (b) pH 6.2. (c) Shift in the minimum conductivity point ($\Delta V_{g,min}$) with the concentration of PSA-ACT complex in the pH 7.4 and pH 6.2 analyte solutions. The $\Delta V_{g,min}$ value was obtained by calculating the difference in $V_{g,min}$ as a reference for the device with no binding of PSA-ACT complex. Adapted from Ref. 54. Reprinted with permission from Elsevier (2013).

oxygen.[99–105] GOx/polyethylenimine-functionlized ionic liquid (PFIL)/RGO electrode has been reported to exhibit DET of GOx and electrocatalytic activity for glucose detection based on oxygen reduction.[104] Negatively charged GOx was immobilized through counter anion exchange from ionic liquid.

DET redox peak at the electrode and its electrocatalytic activity toward O_2 and H_2O_2 were studied using cyclic voltammetric analysis. Based on the high electrocatalytic/reduction activity of the electrode toward O_2 and H_2O_2, an amperometric glucose biosensor was developed. The biosensor showed a linear response in the clinically relevant glucose concentration ranging from 2 to 14 mM. Figure 17 shows the DET peaks at GOx/PFIL/RGO electrode and glucose response based on decrease in oxygen reduction current in response to glucose.

Implantable or wearable glucose biosensors are becoming more popular over strip-based tests in patients where frequent monitoring of glucose is crucial and also strip tests are inconvenient as it involves multiple finger pricking. Atomic thick graphene with unique sensing properties in FET based devices can be easily integrated into miniaturized devices with flexible substrate to develop sensitive and reliable wearable or implanted sensors. Silk fibroin-encapsulated G-FET based enzymatic flexible biosensor has been reported in detection of glucose (Fig. 18).[106]

In this device, silk protein acts as both device substrate and GOx enzyme immobilization material. The biosensing was based upon measuring the differential drain–source current and shift in the dirac point of the graphene in response to doping caused by H_2O_2, the oxidation product of glucose [Fig. 19(a)]. The biosensor showed a linear detection range of 0.01–10 mM of glucose with LOD of 0.1 mM and average sensitivity of 2.5 μA/mM [Fig. 19(b)]. This silk based glucose sensor can be used as a wearable biosensor to measure the glucose from the sweat due to its mechanical flexibility and stability. It can also be implanted in the body for continuous monitoring of glucose as silk is the biocompatible and biodegradable natural polymer. Another similar flexible G-FET glucose biosensor was developed using polyethylene terephthalate (PET) substrate.[107]

https://doi.org/10.1557/jmr.2017.175 Published online by Cambridge University Press

TABLE II. Summary of reports of graphene based biosensors in protein biomarkers detection and their performance.

Graphene based electrode	Biorecognition element	Target	Principle and method of detection	LOD	Application	Reference
Graphene-chitosan/SPCE	Ab1: phosphorylated p53 antibody Ab2: biotin-Ab2 Enzyme label: streptavidin–HRP Substrate: thionine and H_2O_2	Phosphorylated p53 on serine 15 (phospho-p5315)	Sandwich immunoassay; DPV	0.1 ng/mL	POC diagnosis of gamma radiation exposure	84
PTCA/CCG nafion-modified GCE	Aptamer AS1411	Nucleolin on cancer cell surface (HeLa, MDA-231 and K562 cells)	EIS	794 cells/mL (HeLa)	Label-free cancer cell detection	59
3D-G/pDA/Con A	HRP-labeled anti-CEA	CEA	DPV	~90 pg/mL	Tumor biomarker detection	89
Suspended SCG electrode	Antibodies for ANXA2, VEGF, and ENO1	ANXA2, VEGF, and ENO1	*I–V* measurements/ resistance shift measurements	0.1 pg/mL	Lung cancer diagnosis	90
2-ABA/graphene	Anti-cTnI	cTnI	*I–V* measurements/ resistance shift measurements	0.01 ng/mL	Screening and routine monitoring for AMI patient	87
Pt(MPA)-PMA-CVD-EG/GCE	Anti- cTnI Anti-CRP	cTnI CRP	EIS	4.2 pg/mL (cTnI), 8.4 ng/mL (CRP)	Diagnosis of AMI	91 and 92
rGO-TEPA-Pb^{2+} and rGO-TEPA-Cu^{2+}	anti-hsCRP and anti-$sCD40_L$	hsCRP and soluble CD40 ligand	DPV	16.7 (hsCRP) pg/mL, 13.1 pg/mL	Diagnosis for CD	88
GO modified pencil graphite electrode	Thrombin binding aptamer (TBA)	Thrombin	DPV	0.07 nM	Early diagnosis of hemostasis and coagulation abnormalities	93
CVD graphene	Anti-carcinoembryonic antigen	Carcinoembryonic antigen	FET	100 pg/mL	Prognosis and monitor the progress of cancer	94
Aminated graphene amino-PEG covalently linked	An antibody, specific to fibrinogen	Fibrinogen	EIS	500 μg/dL	Trauma-induced coagulopathy	95

SPCE: screen printed carbon electrode, PTCA: 3,4,9,10-perylene tetracarboxylic acid, CCG: chemically converted graphene, 3D G: three dimensional graphene foam, pDA: polydopamine, ConA: concanvaline A, SCG: single crystal graphene, cTnI: cardiac troponin I, 2-ABA: 2-aminobenzyl amine, AMI: acute myocardial infarction, hsCRP: high sensitivity C-reactive protein, TEPA: tetraethylenepentamine, CD: cardiovascular disease, SNAP-25: synaptosomal-associated protein 25, BoNT-LcA: botulinum neurotoxin serotype A light chain, MPA: mercaptopropionic acid, EG: electroactive monolayer graphene.

Compounds like DA, AA, and UA generally coexist in the biological matrices. Since their oxidation potentials are very close to each other, their voltammetric peaks cannot be resolved at traditional bare electrodes. Graphene modified electrodes have been reported in the selective detection of these compounds.[35,108–114] Vertically oriented multilayer graphene nanoflake (MGNF) film with 2–3 nm thick sharp edges possess high electron transfer kinetics and demonstrated well-resolved voltammetric peaks from oxidation of AA, DA, and UA.[35] The biosensing performance of the electrode was measured using DPV as a function of DA concentration and found to be superior to untreated and unmodified carbon electrodes with LOD of 0.17 μM.

Oxidative stress at cellular level has been shown to be an crucial factor in pathogenesis of various diseases such as atherosclerosis,[115] cancer,[116] male infertility[117] etc. Hydrogen peroxide (H_2O_2) is one of the reactive oxygen species (ROS) produced as a by-product of oxidative metabolism *in vivo*. Therefore detection of H_2O_2 is important in clinical diagnosis. Graphene electrodes including RGO,[118,119] single layer graphene nanoplatelets[120] have been reported for DET of hemoglobin, HRP and microperoxidase-11 and H_2O_2 biosensing. To further improve the sensitivity of H_2O_2 biosensing, graphene hybrids have been used with improved surface area for e.g., recently heme peptide-graphene–CNT was shown to have ~15 times more catalytic current for H_2O_2 reduction compared to heme peptide-graphene electrode.[121]

Table III present examples of graphene based electrodes in other metabolites/small molecules sensing.

D. Pathogen biosensing

Detection of pathogens in biological tissues and food samples is of utmost importance in the field of forensics,

https://doi.org/10.1557/jmr.2017.175 Published online by Cambridge University Press

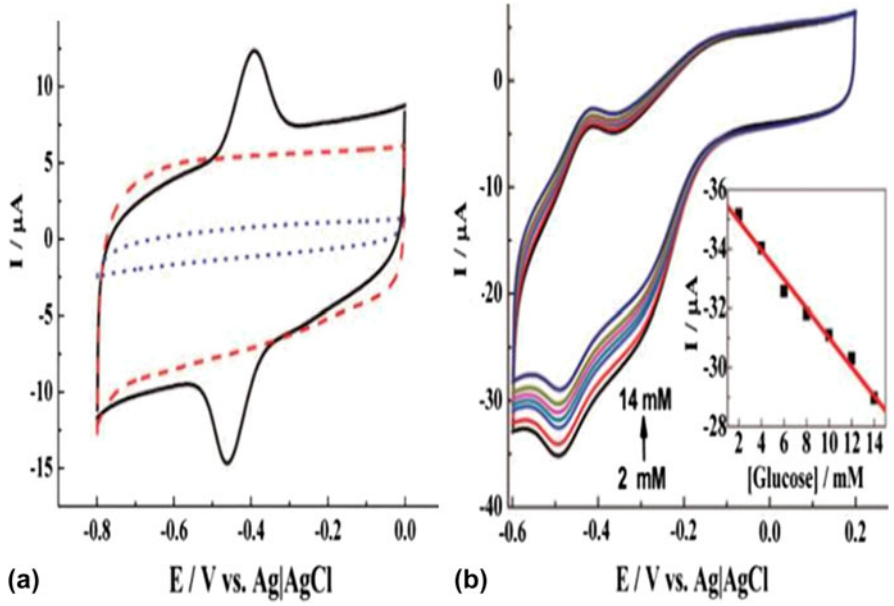


FIG. 17. (a) Cyclic voltammograms of graphene-PFIL (dashed), graphite-GOx-PFIL (dotted), and graphene-GOx-PFIL (solid) modified electrodes in 0.05 M PBS solution (pH = 7.4) saturated with N_2 at a scan rate of 0.05 V/s. (b) Cyclic voltammetric measurements at the graphene-GOx-PFIL modified GC electrode in various concentrations of glucose PBS solution saturated with O_2: 2–14 mM from outer to inner. The inset is the calibration curve (R = 0.994) corresponding to amperometric responses at −0.49 V. Scan rate: 0.05 V/s. Adapted from Ref. 104. Reprinted with permission from American Chemical Society (2009).

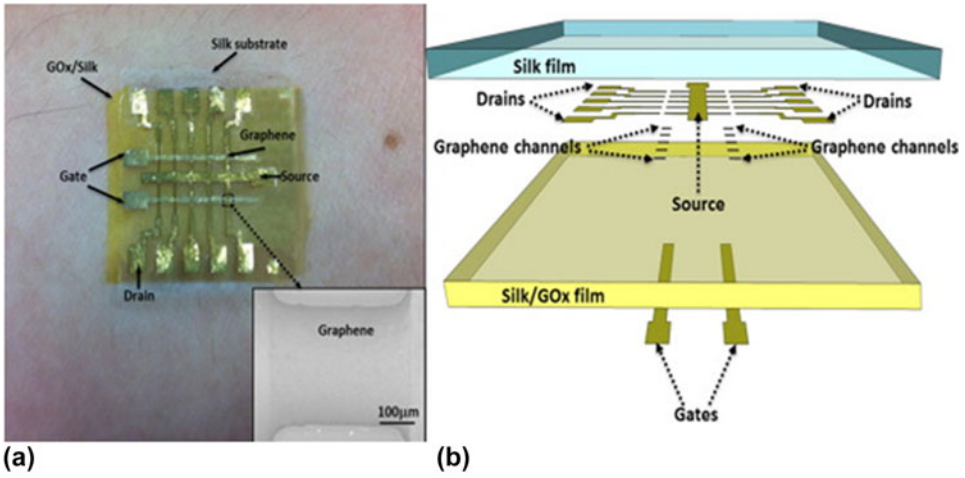


FIG. 18. (a) Optical image of silk-based graphene FET glucose biosensors attached onto the wrist. Each patch contains 10 graphene FET biosensor channels. The inset is an SEM image of a typical graphene FET channel between source and drain electrodes. (b) Exploded-view schematic illustration of the silk-based graphene FET biosensors. Adapted from Ref. 106. Reprinted with permission from Elsevier (2014).

medical diagnostics, and clinical research as it helps in the timely identification and prevention of problems related to health and safety. The conventional techniques to detect microbial pathogens often rely upon clinical microbiology monitoring approaches that are time consuming, expensive and involve labor intensive standard cultures and tests. Hence these methods are inadequate to meet the rapidly growing demands of the industry and cannot be used in situations where managing large numbers of environmental or clinical samples is essential.

TRGO,[130] GO[72,131,132] and CVD graphene[60,133] have been explored in the detection of pathogenic bacteria[60] as well as viruses.[130,131] These bacteria and viruses are specifically captured on the graphene based sensor platform using antibody–antigen interactions. This biospecific binding is then quantified based on the electrical measurements such as current, resistance, or impedance change.

GO produced using chemical exfoliation method produces graphene with irregular edge and shape along with

https://doi.org/10.1557/jmr.2017.175 Published online by Cambridge University Press

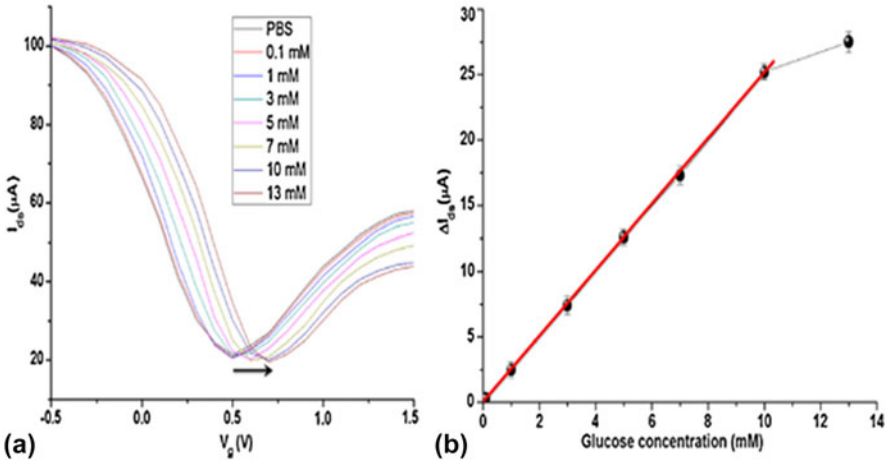


FIG. 19. (a) Charge transfer curves of silk/GOx functionalized graphene FET in response to the addition of glucose to various concentrations at V_{ds} = 100 mV. (b) The response curve of the silk/GOx functionalized graphene FET to glucose at V_g = 0 V. Adapted from Ref. 106. Reprinted with permission from Elsevier (2014).

TABLE III. Examples of graphene based electrodes in other metabolites/small molecules sensing.

Graphene electrode	Analyte	Method of detection	LOD and range of detection	Reference
Hemin-RGO	Tyrosine	CV	75 nM, 0.5–20 μM	122
GO nanoribbons modified SPEs	NADH, dopamine	DPV	0.2 mM, 0.2–7.5 mM (NADH) and 0.004, 0.005–0.8 mM (DA)	123
HRP/sulfonated-G/GC electrode	H_2O_2 and nitrite	DET based detection using cyclic voltammetry	1.17 μM, 3.5–329 μM (H_2O_2) and 19.5, 58.6–488.6 mM	124
ChOx/carboxyl graphene and ChOx/ChEt/carboxyl graphene	Free cholesterol and total cholesterol respectively	Chronoamperometry	5 μM, 50–350 μM (free cholesterol) and 15, 50–300 μM	125
RGO/PSS	Bilirubin	Chronoamperometry	2.0, 0–450 μM	126
ERGO/GCE	Nitric oxide	Chronoamperometry	0.2, 0.72–78.4 μM	127
ERGO deposited on SPCE	L-Lactate	Chronoamperometry	60 μM, 0.5–15 mM	128
ERGO on pencil graphite electrode	Glucose	Chronoamperometry	5.8 μM, 1.0×10^{-5}–1.0×10^{-3} M	129

ChOx: cholesterol oxidase, ChEt: cholesterol esterase, PSS: polystyrene sulfonic acid.

size of GO. These morphological features of graphene greatly affect the electronic properties of graphene therefore the random GO based FET are expected to suffer from low reproducibility. To overcome this issue, micropatterned RGO (MRGO) on the SiO_2/Si substrate was fabricated and integrated in the polydimethylsiloxane (PDMS) microchannel to be applied for label-free, real-time, and ultrasensitive detection of rotavirus.[131] Fig. 20 shows the schematic of an MRGO-FET fabrication.

The rotavirus specific antibody was immobilized on the MRGO-FET through covalent chemistry modifications and then the current (I_0) was stabilized with a PBS buffer. Once the target virus was injected, the relative current change (I) was monitored in real time. Figure 21(a) shows the step by step procedure for detection of rotavirus using MRGO-FET. Concentration of the virus sample was varied from 0 to 10^5 pfu/mL and current drop was measured as shown in Fig. 21(b). As the concentration increased from 0 to 10^5 pfu/mL, the normalized I_d $[(I - I_0)/I_0]$ of the MRGO-FET gradually decreased by 7.23%, 11.06%, 19.0%, 31.45%, 39.0%, and 45.33%, respectively. The current drop was approximately proportional to the virus concentration. The LOD for rotavirus was found to be as 10^2 pfu which is superior to the conventional ELISA method. These results suggest that the MRGO-FET could be used for highly sensitive pathogen detection with improved reproducibility.

In another report, rotavirus was captured on antibody functionalized multilayer free standing TRGO film.[130] The input cell number dependent binding event on the graphene surface was monitored electrochemically using cyclic voltammetry measurements in presence of redox probe. 10^5 pfu/mL and 10^3 pfu/mL of input cells were detected with approximately 30.7% and 1.3% sensitivity respectively demonstrating application of TRGO for electrochemical biosensing of rotavirus.

CVD grown G-based biosensor for a fast, label-free, and selective detection of bacteria *E. coli* with high

https://doi.org/10.1557/jmr.2017.175 Published online by Cambridge University Press

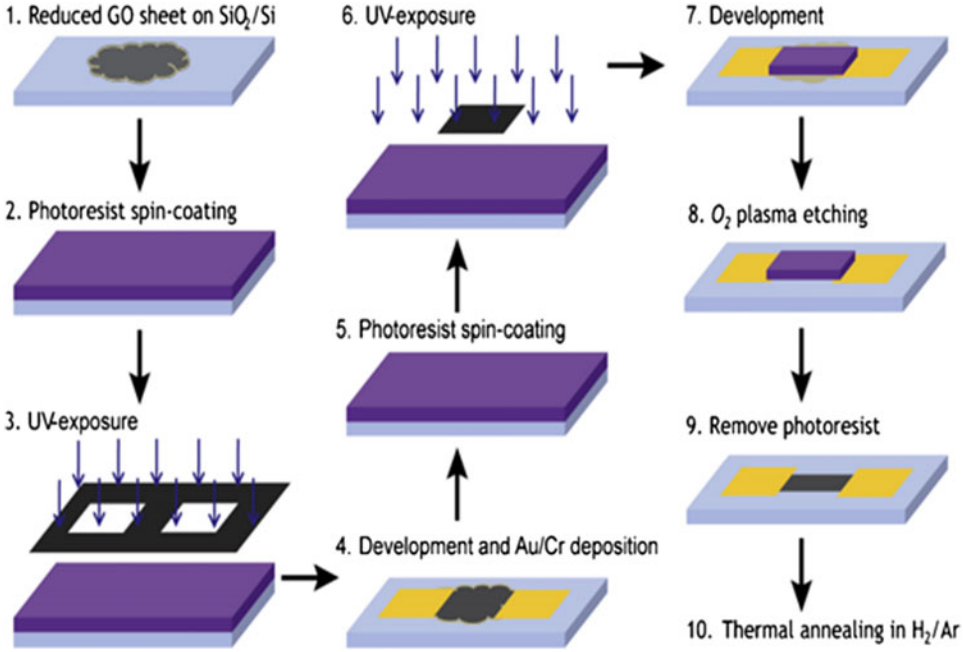


FIG. 20. Schematic illustration for fabricating an MRGO-FET. Adapted from Ref. 131. Reprinted with permission from Elsevier (2013).

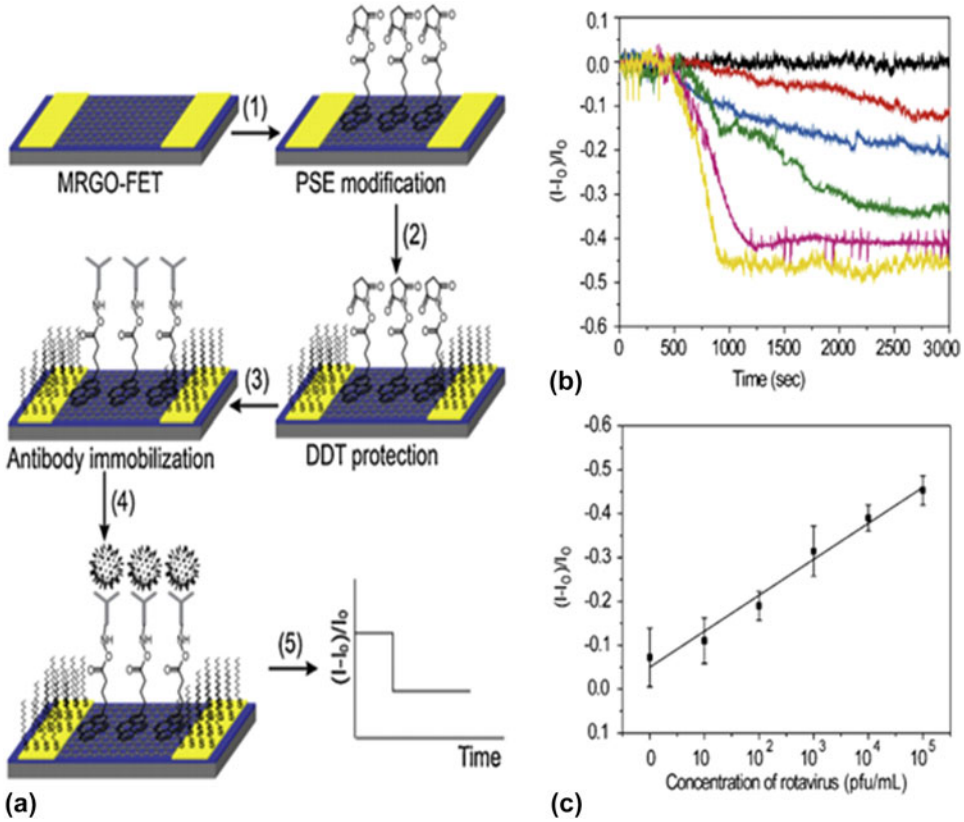


FIG. 21. (a) Schematics of the MRGO-FET based rotavirus detection. (1) 1-Pyrenebutyric acid *N*-hydroxysuccinimide ester (PSE) modification, (2) blocking of the gold electrode by 1-dodecanethiol (DDT), (3) antibody immobilization and blocking the MRGO surface by ethanolamine, (4) rotavirus capture and (5) electrical signal detection. (b) Real-time and label-free virus detection on the MRGO-FET device at $V_{ds} = 0.1$ V. (b) Current response of the MRGO-FET device depending on the concentration of a rotavirus sample [blank (black), 10 (red), 10^2 (blue), 10^3 (green), 10^4 (pink), and 10^5 pfu/mL (yellow)], (c) calibration plot of the detection. Adapted from Ref. 131. Reprinted with permission from Elsevier (2013).

https://doi.org/10.1557/jmr.2017.175 Published online by Cambridge University Press

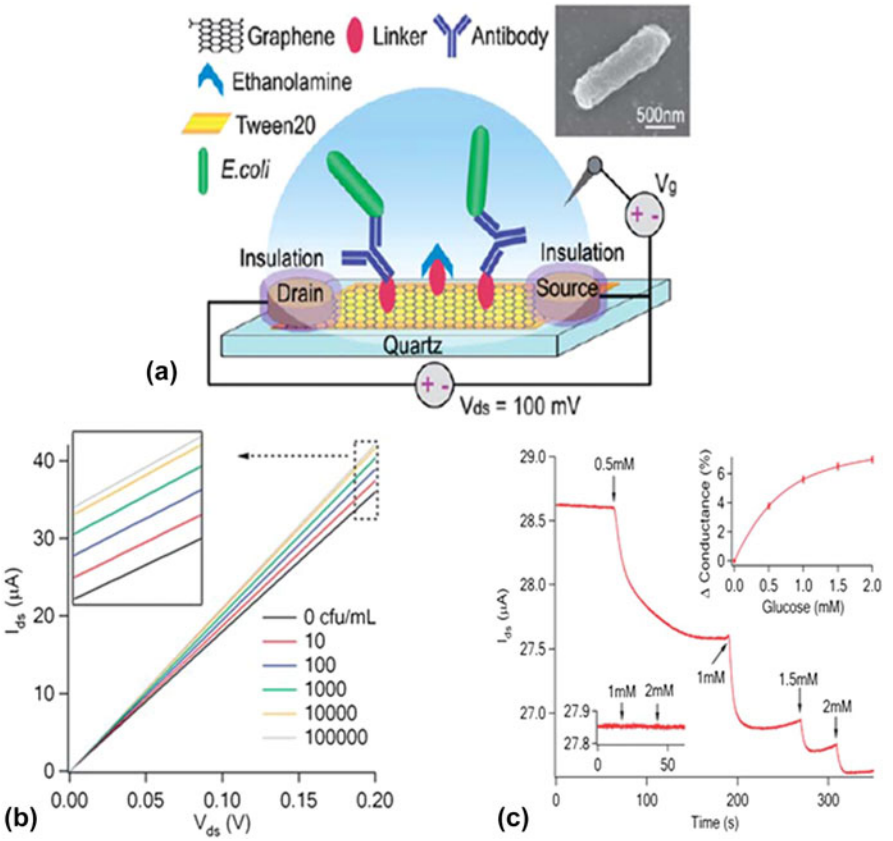


FIG. 22. (a) Illustration of anti-*E. coli* antibody functionalized graphene-FET for detection of *E. coli*. Inset: scanning electron microscopy (SEM) image of an *E. coli* on antibody functionalized graphene. (b) I_{ds} versus V_{ds} curves of anti-*E. coli* antibody functionalized graphene device after incubated with *E. coli* of different concentrations. $V_g = 0$ V. (c) Real-time current recording ($V_{ds} = 100$ mV and $V_g = 0$ V) of a graphene device immobilized with *E. coli* bacteria with addition of glucose to the PBS recording buffer at the indicated time points to reach the final concentrations of 0.5, 1, 1.5, and 2 mM. Adapted from Ref. 60 with permission of The Royal Society of Chemistry (2011).

TABLE IV. Summary of the recently reported pathogen biosensors using graphene based electrodes.

Graphene electrode	Target pathogen	Method of detection	LOD and range of detection	Reference
Micropatterned RGO	Rotavirus	FET	10^2 pfu/mL; 0 to 10^5 pfu/mL	131
Anti-*E. coli*/CVD graphene	*E. coli*	FET	10 cfu/mL	60
Multilayer free standing TRGO film	Rotavirus	Cyclic voltammetry	10^3 pfu/mL; linear range of detection 10–10^3 pfu	130
RGO/Au	Botulinum neurotoxin A	DPV	1 pg/mL; linear detection range from 1 pg/mL to 1 ng/mL	134
poly[G]20 biobarcode NPs-(GO-COOH)	Uropathogens	Square wave voltammograms	1 pM	132
Graphene-silk fibroin	*E. coli*, *H. pylori* and *S. aureus*	Wireless monitoring of resistance change	~100 cells; upto 10^6 cells	133
Reduced graphene sheets (RGSs)-doped chitosan (CS) nanocomposite film	Marine pathogenic sulfate-reducing bacteria (SRB)	EIS	1.8×10^1–1.8×10^7 cfu/mL	135
CVD graphene 3D printed on flexible Kapton substrate	The foodborne pathogen, norovirus	FET	0.1 μg/mL	136
Graphene nanosheet	Cholera toxin	Potentiometry	1 nM	137
Reduced GO nanogrids	Hepatitis B virus	FET	50 aM	138

sensitivity (10 cfu/mL) and specificity was reported.[60] Fig. 22(a) shows the schematics of anti-*E. coli* antibody functionalized graphene-FET for detection of *E. coli* biosensor. The binding of *E. coli* to its specific antibodies immobilized on the graphene electrode and subsequent increase in the conductance was recorded

https://doi.org/10.1557/jmr.2017.175 Published online by Cambridge University Press

[Fig. 22(b)]. The anti-*E. coli* functionalized G-FET was found to be pH sensitive and also studied for real time detection of metabolic activities of *E. coli* triggered by glucose [Fig. 22(c)]. This nanoelectronic biosensor could serve as a high throughput platform for fast and reliable detection of any pathogenic bacteria, and for functional studies or screening of antibacterial drugs.

Table IV is a summary of the recently reported pathogen biosensors using graphene based electrodes.

V. SUMMARY

In summary, exceptional electrical and chemical properties of graphene and its derivatives provide an ideal platform for the development of reliable and highly sensitive sensors for healthcare. This chapter comprehensively discusses the synthesis of such structures and their functionalization for fabricating electrochemical sensors that help detect a wide array of biological entities such as DNA, proteins, and pathogens with enhanced sensitivity and specificity. Research on the interface of graphene and a variety of materials such as metals, metal oxides, polymers, quantum dots, and small molecules is emerging as one of the most dynamic areas in healthcare research as it establishes excellent coupling with bio-entities that forms the basis of developing efficient, long lasting sensors for detection of a multitude of diseases, toxins, and biomarkers. It is indeed without any doubt that given the unique selling point of graphene, such research will proliferate into related areas of medicine, drug/gene delivery, cancer therapies, and other biomedical applications.

ACKNOWLEDGMENT

We acknowledge the financial support of the National Science Foundation (1307671), U.S. Department of Agriculture (2014-67021-21589), and W. Ruel Johnson Chair in Environmental Engineering.

REFERENCES

1. E. Fitzer, K.H. Kochling, H.P. Boehm, and H. Marsh: Recommended terminology for the description of carbon as a solid—(iupac recommendations 1995). *Pure Appl. Chem.* **67**, 473 (1995).
2. K.S. Novoselov, A.K. Geim, S.V. Morozov, D. Jiang, Y. Zhang, S.V. Dubonos, I.V. Grigorieva, and A.A. Firsov: Electric field effect in atomically thin carbon films. *Science* **306**, 666 (2004).
3. D.R. Dreyer, S. Park, C.W. Bielawski, and R.S. Ruoff: The chemistry of graphene oxide. *Chem. Soc. Rev.* **39**, 228 (2010).
4. A.J. Vanbommel, J.E. Crombeen, and A. Vantooren: Leed and auger-electron observations of SIC (0001) surface. *Surf. Sci.* **48**, 463 (1975).
5. W.A. de Heer, C. Berger, M. Ruan, M. Sprinkle, X. Li, Y. Hu, B. Zhang, J. Hankinson, and E. Conrad: Large area and structured epitaxial graphene produced by confinement controlled sublimation of silicon carbide. *Proc. Natl. Acad. Sci. U. S. A.* **108**, 16900 (2011).
6. C. Berger, Z. Song, X. Li, X. Wu, N. Brown, C. Naud, D. Mayou, T. Li, J. Hass, A.N. Marchenkov, E.H. Conrad, P.N. First, and W.A. de Heer: Electronic confinement and coherence in patterned epitaxial graphene. *Science* **312**, 1191 (2006).
7. J. Hass, W.A. de Heer, and E.H. Conrad: The growth and morphology of epitaxial multilayer graphene. *J. Phys.: Condens. Matter* **20**, 323202 (2008).
8. P.N. First, W.A. de Heer, T. Seyller, C. Berger, J.A. Stroscio, and J.-S. Moon: Epitaxial graphenes on silicon carbide. *MRS Bull.* **35**, 296 (2010).
9. R. Zan, Q.M. Ramasse, R. Jalil, and U. Bangert: Atomic structure of graphene and h-BN layers and their interactions with metals. In *Adv. Graphene Sci.* (INTECH, 2013).
10. H. Bai, C. Li, and G. Shi: Functional composite materials based on chemically converted graphene. *Adv. Mater.* **23**, 1089 (2011).
11. P. Marques, G. Gonçalves, S. Cruz, N. Almeida, M. Singh, J. Grácio, and A. Sousa: Functionalized graphene nanocomposites. In *Adv. Nanocomposite Tech.*, A. Hashim, ed. (INTECH, 2011).
12. P.W. Sutter, J-I. Flege, and E.A. Sutter: Epitaxial graphene on ruthenium. *Nat. Mater.* **7**, 406 (2008).
13. A. Kumar, and C. H. Lee: Synthesis and Biomedical Applications of Graphene: Present and Future Trends. In *Adv. Graphene Sci.*, M. Aliofkhazraei, ed. (INTECH, 2013).
14. M. Losurdo, M.M. Giangregorio, P. Capezzuto, and G. Bruno: Graphene CVD growth on copper and nickel: Role of hydrogen in kinetics and structure. *Phys. Chem. Chem. Phys.* **13**, 20836 (2011).
15. H.L. Zhou, W.J. Yu, L.X. Liu, R. Cheng, Y. Chen, X.Q. Huang, Y. Liu, Y. Wang, Y. Huang, and X.F. Duan: Chemical vapour deposition growth of large single crystals of monolayer and bilayer graphene. *Nat. Commun.* **4**, 2096 (2013).
16. L. Huang, Q.H. Chang, G.L. Guo, Y. Liu, Y.Q. Xie, T. Wang, B. Ling, and H.F. Yang: Synthesis of high-quality graphene films on nickel foils by rapid thermal chemical vapor deposition. *Carbon* **50**, 551–556 (2012).
17. Y. Zhang, M. Ma, J. Yang, W. Huang, and X. Dong: Graphene-based three-dimensional hierarchical sandwich-type architecture for high performance supercapacitors. *RSC Adv.* **4**, 8466 (2014).
18. S.Y. Yang, J.G. Oh, D.Y. Jung, H. Choi, C.H. Yu, J. Shin, C.-G. Choi, B.J. Cho, and S.-Y. Choi: Metal-etching-free direct delamination and transfer of single-layer graphene with a high degree of freedom. *Small* **11**, 175 (2015).
19. W. Regan, N. Alem, B. Aleman, B. Geng, C. Girit, L. Maserati, F. Wang, M. Crommie, and A. Zettl: A direct transfer of layer-area graphene. *Appl. Phys. Lett.* **96**, 113102 (2010).
20. A.V. Zaretski, H. Moetazedi, C. Kong, E.J. Sawyer, S. Savagatrup, E. Valle, T.F. O'Connor, A.D. Printz, and D.J. Lipomi: Metal-assisted exfoliation (MAE): Green, roll-to-roll compatible method for transferring graphene to flexible substrates. *Nanotechnology* **26**, 045301 (2015).
21. D.A.C. Brownson, D.K. Kampouris, and C.E. Banks: Graphene electrochemistry: Fundamental concepts through to prominent applications. *Chem. Soc. Rev.* **41**, 6944 (2012).
22. S. Badhulika, T. Terse-Thakoor, C.M. Chaves Villarreal, and A. Mulchandani: Graphene hybrids: Synthesis strategies and applications in sensors and sensitized solar cells. *Front. Chem.* **3**, 38 (2015).
23. X. Yang, X. Dou, A. Rouhanipour, L. Zhi, H.J. Raeder, and K. Muellen: Two-dimensional graphene nanoribbons. *J. Am. Chem. Soc.* **130**(13), 4216 (2008).
24. M.Y. Han, B. Oezyilmaz, Y. Zhang, and P. Kim: Energy band-gap engineering of graphene nanoribbons. *Phys. Rev. Lett.* **98**, 206805 (2007).
25. J. Cai, P. Ruffieux, R. Jaafar, M. Bieri, T. Braun, S. Blankenburg, M. Muoth, A.P. Seitsonen, M. Saleh, X. Feng, K. Muellen, and

https://doi.org/10.1557/jmr.2017.175 Published online by Cambridge University Press

R. Fasel: Atomically precise bottom-up fabrication of graphene nanoribbons. *Nature* **466**, 470–473 (2010).
26. D.V. Kosynkin, A.L. Higginbotham, A. Sinitskii, J.R. Lomeda, A. Dimiev, B.K. Price, and J.M. Tour: Longitudinal unzipping of carbon nanotubes to form graphene nanoribbons. *Nature* **458**, 872 (2009).
27. L. Jiao, L. Zhang, X. Wang, G. Diankov, and H. Dai: Narrow graphene nanoribbons from carbon nanotubes. *Nature* **458**, 877 (2009).
28. D. Sarkar, W. Liu, X. Xie, A.C. Anselmo, S. Mitragotri, and K. Banerjee: MoS_2 field-effect transistor for next-generation label-free biosensors. *ACS Nano* **8**, 3992 (2014).
29. L. Jiao, X. Wang, G. Diankov, H. Wang, and H. Dai: Facile synthesis of high-quality graphene nanoribbons. *Nat. Nanotechnol.* **5**, 321 (2010).
30. X. Wang, Y. Ouyang, L. Jiao, H. Wang, L. Xie, J. Wu, J. Guo, and H. Dai: Graphene nanoribbons with smooth edges behave as quantum wires. *Nat. Nanotechnol.* **6**, 563 (2011).
31. D.B. Shinde, J. Debgupta, A. Kushwaha, M. Aslam, and V.K. Pillai: Electrochemical unzipping of multi-walled carbon nanotubes for facile synthesis of high-quality graphene nanoribbons. *J. Am. Chem. Soc.* **133**, 4168 (2011).
32. Y.H. Wu, P.W. Qiao, T.C. Chong, and Z.X. Shen: Carbon nanowalls grown by microwave plasma enhanced chemical vapor deposition. *Adv. Mater.* **14**, 64 (2002).
33. S. Suzuki, A. Chatterjee, C-L. Cheng, and M. Yoshimura: Effect of hydrogen on carbon nanowall growth by microwave plasma-enhanced chemical vapor deposition. *Jpn. J. Appl. Phys.* **50**, 01AF08 (2011).
34. K. Tanaka, M. Yoshimura, A. Okamoto, and K. Ueda: Growth of carbon nanowalls on a SiO_2 substrate by microwave plasma-enhanced chemical vapor deposition. *Jpn. J. Appl. Phys., Part 1* **44**, 2074 (2005).
35. N.G. Shang, P. Papakonstantinou, M. McMullan, M. Chu, A. Stamboulis, A. Potenza, S.S. Dhesi, and H. Marchetto: Catalyst-free efficient growth, orientation and biosensing properties of multilayer graphene nanoflake films with sharp edge planes. *Adv. Funct. Mater.* **18**, 3506 (2008).
36. K. Davami, M. Shaygan, N. Kheirabi, J. Zhao, D.A. Kovalenko, M.H. Ruemmeli, J. Opitz, G. Cuniberti, J.-S. Lee, and M. Meyyappan: Synthesis and characterization of carbon nanowalls on different substrates by radio frequency plasma enhanced chemical vapor deposition. *Carbon* **72**, 372 (2014).
37. H.G. Jain, H. Karacuban, D. Krix, H.-W. Becker, H. Nienhaus, and V. Buck: Carbon nanowalls deposited by inductively coupled plasma enhanced chemical vapor deposition using aluminum acetylacetonate as precursor. *Carbon* **49**, 4987 (2011).
38. S. Kondo, M. Hori, K. Yamakawa, S. Den, H. Kano, and M. Hiramatsu: Highly reliable growth process of carbon nanowalls using radical injection plasma-enhanced chemical vapor deposition. *J. Vac. Sci. Technol., A* **26**, 1294 (2008).
39. M. Hiramatsu, K. Shiji, H. Amano, and M. Hori: Fabrication of vertically aligned carbon nanowalls using capacitively coupled plasma-enhanced chemical vapor deposition assisted by hydrogen radical injection. *Appl. Phys. Lett.* **84**, 4708 (2004).
40. S.Y. Kim, Y.H. Joung, and W.S. Choi: Growth properties of carbon nanowalls on glass substrates by a microwave plasma-enhanced chemical vapor deposition. *Jpn. J. Appl. Phys.* **53**, 05FD09 (2014).
41. J. Fang, I. Levchenko, S. Kumar, D. Seo, and K. Ostrikov: Vertically-aligned graphene flakes on nanoporous templates: Morphology, thickness, and defect level control by pre-treatment. *Sci. Technol. Adv. Mater.* **15**, 055009 (2014).
42. P. Kumar Roy, A. Ganguly, W.-H. Yang, C.-T. Wu, J.-S. Hwang, Y. Tai, K.-H. Chen, L.-C. Chen, and S. Chattopadhyay: Edge promoted ultrasensitive electrochemical detection of organic biomolecules on epitaxial graphene nanowalls. *Biosens. Bioelectron.* **70**, 137 (2015).
43. O. Akhavan, E. Ghaderi, and R. Rahighi: Toward single-DNA electrochemical biosensing by graphene nanowalls. *ACS Nano* **6**, 2904 (2012).
44. O. Akhavan, E. Ghaderi, E. Hashemi, and R. Rahighi: Ultra-sensitive detection of leukemia by graphene. *Nanoscale* **6**, 14810 (2014).
45. T. Yang, Q. Guan, L. Meng, R. Yang, Q. Li, and K. Jiao: A simple preparation method for large-area, wavy graphene oxide nanowalls and their application to freely switchable impedimetric DNA detection. *RSC Adv.* **3**, 22430 (2013).
46. X. Dong, Q. Long, J. Wang, M.B. Chan-Park, Y. Huang, W. Huang, and P. Chen: A graphene nanoribbon network and its biosensing application. *Nanoscale* **3**, 5156 (2011).
47. Y. Hu, F. Li, X. Bai, D. Li, S. Hua, K. Wang, and L. Niu: Label-free electrochemical impedance sensing of DNA hybridization based on functionalized graphene sheets. *Chem. Commun.* **47**, 1743 (2011).
48. Y. Hu, F. Li, D. Han, T. Wu, Q. Zhang, L. Niu, and Y. Bao: Simple and label-free electrochemical assay for signal-on DNA hybridization directly at undecorated graphene oxide. *Anal. Chim. Acta* **753**, 82 (2012).
49. A. Singh, G. Sinsinbar, M. Choudhary, V. Kumar, R. Pasricha, H.N. Verma, S.P. Singh, and K. Arora: Graphene oxide-chitosan nanocomposite based electrochemical DNA biosensor for detection of typhoid. *Sens. Actuators, B* **185**, 675 (2013).
50. Y. Qiu, X. Qu, J. Dong, S. Ai, and R. Han: Electrochemical detection of DNA damage induced by acrylamide and its metabolite at the graphene-ionic liquid-Nafion modified pyrolytic graphite electrode. *J. Hazard. Mater.* **190**, 480 (2011).
51. M. Giovanni, A. Bonanni, and M. Pumera: Detection of DNA hybridization on chemically modified graphene platforms. *Analyst* **137**, 580 (2012).
52. A-M.J. Haque, H. Park, D. Sung, S. Jon, S.-Y. Choi, and K. Kim: An electrochemically reduced graphene oxide-based electrochemical immunosensing platform for ultrasensitive antigen detection. *Anal. Chem.* **84**, 1871 (2012).
53. T.N. Truong: Development of label-free impedimetric Hcg-immunosensor using screen-printed electrode. *J. Biosens. Bioelectron.* **2**(3), 1000107 (2011).
54. D-J. Kim, I.Y. Sohn, J.-H. Jung, O.J. Yoon, N.E. Lee, and J.-S. Park: Reduced graphene oxide field-effect transistor for label-free femtomolar protein detection. *Biosens. Bioelectron.* **41**, 621 (2013).
55. Y.Z. Zhang, T. Liu, B. Meng, X.H. Li, G.Z. Liang, X.N. Hu, and Q.J. Wang: Broadband high photoresponse from pure monolayer graphene photodetector. *Nat. Commun.* **4**, 1811 (2013).
56. X. Dong, Y. Shi, W. Huang, P. Chen, and L-J. Li: Electrical detection of DNA hybridization with single-base specificity using transistors based on CVD-grown graphene sheets. *Adv. Mater.* **22**, 1649 (2010).
57. C-T. Lin, L. Phan Thi Kim, T.-Y. Chen, K.-K. Liu, C.-H. Chen, K.-H. Wei, and L.-J. Li: Label-free electrical detection of DNA hybridization on graphene using Hall effect measurements: Revisiting the sensing mechanism. *Adv. Funct. Mater.* **23**, 2301 (2013).
58. Q. Gong, H. Yang, Y. Dong, and W. Zhang: A sensitive impedimetric DNA biosensor for the determination of the HIV gene based on electrochemically reduced graphene oxide. *Anal. Methods* **7**, 2554 (2015).
59. L. Feng, Y. Chen, J. Ren, and X. Qu: A graphene functionalized electrochemical aptasensor for selective label-free detection of cancer cells. *Biomaterials* **32**, 2930 (2011).

https://doi.org/10.1557/jmr.2017.175 Published online by Cambridge University Press

60. Y. Huang, X. Dong, Y. Liu, L-J. Li, and P. Chen: Graphene-based biosensors for detection of bacteria and their metabolic activities. *J. Mater. Chem.* **21**, 12358 (2011).
61. J.C. Liao, M. Mastali, Y. Li, V. Gau, M.A. Suchard, J. Babbitt, J. Gornbein, E.M. Landaw, E.R.B. McCabe, B.M. Churchill, and D.A. Haake: Development of an advanced electrochemical DNA biosensor for bacterial pathogen detection. *J. Mol. Diagn.* **9**, 158 (2007).
62. F. Lucarelli, G. Marrazza, A.P.F. Turner, and M. Mascini: Carbon and gold electrodes as electrochemical transducers for DNA hybridisation sensors. *Biosens. Bioelectron.* **19**, 515 (2004).
63. J.C. Liao, M. Mastali, V. Gau, M.A. Suchard, A.K. Moller, D.A. Bruckner, J.T. Babbitt, Y. Li, J. Gornbein, E.M. Landaw, E.R.B. McCabe, B.M. Churchill, and D.A. Haake: Use of electrochemical DNA biosensors for rapid molecular identification of uropathogens in clinical urine specimens. *J. Clin. Microbiol.* **44**, 561 (2006).
64. T.G. Drummond, M.G. Hill, and J.K. Barton: Electrochemical DNA sensors. *Nat. Biotechnol.* **21**, 1192 (2003).
65. S.C.B. Oliveira and A.M. Oliveira-Brett: DNA-electrochemical biosensors: AFM surface characterisation and application to detection of *in situ* oxidative damage to DNA. *Comb. Chem. High Throughput Screening* **13**, 628 (2010).
66. E. Palecek, M. Fojta, M. Tomschik, and J. Wang: Electrochemical biosensors for DNA hybridization and DNA damage. *Biosens. Bioelectron.* **13**, 621 (1998).
67. J. Wang: From DNA biosensors to gene chips. *Nucleic Acids Res.* **28**, 3011 (2000).
68. S. Akca, A. Foroughi, D. Frochtzwajg, and H.W.C. Postma: Competing interactions in DNA assembly on graphene. *PLoS One* **6**(4), e18442 (2011).
69. A. Bonanni and M. Pumera: Graphene platform for hairpin-DNA-based impedimetric genosensing. *ACS Nano* **5**, 2356 (2011).
70. B. Esteban-Fernandez de Avila, E. Araque, S. Campuzano, M. Pedrero, B. Dalkiran, R. Barderas, R. Villalonga, E. Kilic, and J.M. Pingarron: Dual functional graphene derivative-based electrochemical platforms for detection of the TP53 gene with single nucleotide polymorphism selectivity in biological samples. *Anal. Chem.* **87**, 2290 (2015).
71. C.X. Lim, H.Y. Hoh, P.K. Ang, and K.P. Loh: Direct voltammetric detection of DNA and pH sensing on epitaxial graphene: An insight into the role of oxygenated defects. *Anal. Chem.* **82**, 7387 (2010).
72. N. Mohanty and V. Berry: Graphene-based single-bacterium resolution biodevice and DNA transistor: Interfacing graphene derivatives with nanoscale and microscale biocomponents. *Nano Lett.* **8**, 4469 (2008).
73. Z. Wang, J. Zhang, P. Chen, X. Zhou, Y. Yang, S. Wu, L. Niu, Y. Han, L. Wang, F. Boey, Q. Zhang, B. Liedberg, and H. Zhang: Label-free, electrochemical detection of methicillin-resistant *Staphylococcus aureus* DNA with reduced graphene oxide-modified electrodes. *Biosens. Bioelectron.* **26**, 3881 (2011).
74. Y. Hu, K. Wang, Q. Zhang, F. Li, T. Wu, and L. Niu: Decorated graphene sheets for label-free DNA impedance biosensing. *Biomaterials* **33**, 1097 (2012).
75. L-P. Jia, J-F. Liu, and H-S. Wang: Electrochemical performance and detection of 8-hydroxy-2′-deoxyguanosine at single-stranded DNA functionalized graphene modified glassy carbon electrode. *Biosens. Bioelectron.* **67**, 139 (2015).
76. M. Du, T. Yang, X. Li, and K. Jiao: Fabrication of DNA/graphene/polyaniline nanocomplex for label-free voltammetric detection of DNA hybridization. *Talanta* **88**, 439 (2012).
77. B. Li, G. Pan, N.D. Avent, R.B. Lowry, T.E. Madgett, and P.L. Waines: Graphene electrode modified with electrochemically reduced graphene oxide for label-free DNA detection. *Biosens. Bioelectron.* **72**, 313 (2015).
78. A. Benvidi, N. Rajabzadeh, M. Mazloum-Ardakani, M.M. Heidari, and A. Mulchandani: Simple and label-free electrochemical impedance Amelogenin gene hybridization biosensing based on reduced graphene oxide. *Biosens. Bioelectron.* **58**, 145 (2014).
79. O. Akhavan, E. Ghaderi, R. Rahighi, and M. Abdolahad: Spongy graphene electrode in electrochemical detection of leukemia at single-cell levels. *Carbon* **79**, 654 (2014).
80. Q.J. Gong, Y.D. Wang, and H.Y. Yang: A sensitive impedimetric DNA biosensor for the determination of the HIV gene based on graphene-Nafion composite film. *Biosens. Bioelectron.* **89**, 565 (2017).
81. A. Seidel, S. Brunner, P. Seidel, G.I. Fritz, and O. Herbarth: Modified nucleosides: An accurate tumour marker for clinical diagnosis of cancer, early detection and therapy control. *Br. J. Cancer* **94**, 1726 (2006).
82. E. Borek, O.K. Sharma, F.L. Buschman, D.L. Cohn, K.A. Penley, F.N. Judson, B.S. Dobozin, C.R. Horsburgh, and C.H. Kirkpatrick: Altered excretion of modified nucleosides and beta-aminoisobutyric acid in subjects with acquired-immunodeficiency-syndrome or at risk for acquired-immunodeficiency-syndrome. *Cancer Res.* **46**, 2557 (1986).
83. K-J. Huang, D.-J. Niu, J.-Y. Sun, C.-H. Han, Z.-W. Wu, Y.-L. Li, and X.-Q. Xiong: Novel electrochemical sensor based on functionalized graphene for simultaneous determination of adenine and guanine in DNA. *Colloids Surf., B* **82**, 543 (2011).
84. Y. Xie, A. Chen, D. Du, and Y. Lin: Graphene-based immunosensor for electrochemical quantification of phosphorylated p53 (S15). *Anal. Chim. Acta* **699**, 44 (2011).
85. D. Du, L. Wang, Y. Shao, J. Wang, M.H. Engelhard, and Y. Lin: Functionalized graphene oxide as a nanocarrier in a multienzyme labeling amplification strategy for ultrasensitive electrochemical immunoassay of phosphorylated p53 (S392). *Anal. Chem.* **83**, 746 (2011).
86. X. Chen, X. Jia, J. Han, J. Ma, and Z. Ma: Electrochemical immunosensor for simultaneous detection of multiplex cancer biomarkers based on graphene nanocomposites. *Biosens. Bioelectron.* **50**, 356 (2013).
87. S.K. Tuteja, M. Kukkar, C.R. Suri, A.K. Paul, and A. Deep: One step *in situ* synthesis of amine functionalized graphene for immunosensing of cardiac marker cTnI. *Biosens. Bioelectron.* **66**, 129 (2015).
88. G. Yuan, C. Yu, C. Xia, L. Gao, W. Xu, W. Li, and J. He: A simultaneous electrochemical multianalyte immunoassay of high sensitivity C-reactive protein and soluble CD40 ligand based on reduced graphene oxide-tetraethylene pentamine that directly adsorb metal ions as labels. *Biosens. Bioelectron.* **72**, 237 (2015).
89. J. Liu, J. Wang, T. Wang, D. Li, F. Xi, J. Wang, and E. Wang: Three-dimensional electrochemical immunosensor for sensitive detection of carcinoembryonic antigen based on monolithic and macroporous graphene foam. *Biosens. Bioelectron.* **65**, 281 (2015).
90. P. Li, B. Zhang, and T. Cui: Towards intrinsic graphene biosensor: A label-free, suspended single crystalline graphene sensor for multiplex lung cancer tumor markers detection. *Biosens. Bioelectron.* **72**, 168 (2015).
91. S. Singal, A.K. Srivastava, A.M. Biradar, A. Mulchandani, and Rajesh: Pt nanoparticles-chemical vapor deposited graphene composite based immunosensor for the detection of human cardiac troponin I. *Sens. Actuators, B* **205**, 363 (2014).

https://doi.org/10.1557/jmr.2017.175 Published online by Cambridge University Press

92. S. Singal, A.M. Biradar, A. Mulchandani, and Rajesh: Ultrasensitive electrochemical immunosensor based on Pt nanoparticle–graphene composite. *Appl. Biochem. Biotechnol.* **174**, 971 (2014).
93. F. Ahour and M.K. Ahsani: An electrochemical label-free and sensitive thrombin aptasensor based on graphene oxide modified pencil graphite electrode. *Biosens. Bioelectron.* **86**, 764 (2016).
94. L. Zhou, H.J. Mao, C.Y. Wu, L. Tang, Z.H. Wu, H. Sun, H.L. Zhang, H.B. Zhou, C.P. Jia, Q.H. Jin, X.F. Chen, and J.L. Zhao: Label-free graphene biosensor targeting cancer molecules based on non-covalent modification. *Biosens. Bioelectron.* **87**, 701 (2017).
95. W. Saleem, C. Salinas, B. Watkins, G. Garvey, A.C. Sharma, and R. Ghosh: Antibody functionalized graphene biosensor for label-free electrochemical immunosensing of fibrinogen, an indicator of trauma induced coagulopathy. *Biosens. Bioelectron.* **86**, 522 (2016).
96. M. Harris: Classification and diagnosis of diabetes-mellitus and other categories of glucose-intolerance. *Diabetes* **28**, 1039 (1979).
97. R. Mohandas and R.J. Johnson: Uric acid levels increase risk for new-onset kidney disease. *J. Am. Soc. Nephrol.* **19**, 2251 (2008).
98. R.M. Wightman, L.J. May, and A.C. Michael: Detection of dopamine dynamics in the brain. *Anal. Chem.* **60**, A769 (1988).
99. P. Wu, Q. Shao, Y. Hu, J. Jin, Y. Yin, H. Zhang, and C. Cai: Direct electrochemistry of glucose oxidase assembled on graphene and application to glucose detection. *Electrochim. Acta* **55**, 8606 (2010).
100. K. Xinhuang, W. Jun, W. Hong, I.A. Aksay, L. Jun, and L. Yuehe: Glucose oxidase-graphene-chitosan modified electrode for direct electrochemistry and glucose sensing. *Biosens. Bioelectron.* **25**, 901 (2009).
101. Q. Zhang, S. Wu, L. Zhang, J. Lu, F. Verproot, Y. Liu, Z. Xing, J. Li, and X.-M. Song: Fabrication of polymeric ionic liquid/graphene nanocomposite for glucose oxidase immobilization and direct electrochemistry. *J. Biosens. Bioelectron.* **26**, 2632 (2011).
102. C. Fu, W. Yang, X. Chen, and D.G. Evans: Direct electrochemistry of glucose oxidase on a graphite nanosheet-Nafion composite film modified electrode. *Electrochem. Commun.* **11**, 997 (2009).
103. S. Alwarappan, S.R. Singh, S. Pillai, A. Kumar, and S. Mohapatra: Direct electrochemistry of glucose oxidase at a gold electrode modified with graphene nanosheets. *Anal. Lett.* **45**, 746 (2012).
104. C. Shan, H. Yang, J. Song, D. Han, A. Ivaska, and L. Niu: Direct electrochemistry of glucose oxidase and biosensing for glucose based on graphene. *Anal. Chem.* **81**, 2378 (2009).
105. B. Unnikrishnan, S. Palanisamy, and S-M. Chen: A simple electrochemical approach to fabricate a glucose biosensor based on graphene–glucose oxidase biocomposite. *Biosens. Bioelectron.* **39**, 70 (2013).
106. Y. Xueqiu and J.J. Pak: Graphene-based field effect transistor enzymatic glucose biosensor using silk protein for enzyme immobilization and device substrate. *Sens. Actuators, B* **202**, 1357 (2014).
107. Y.H. Kwak, D.S. Choi, Y.N. Kim, H. Kim, D.H. Yoon, S.-S. Ahn, J.-W. Yang, W.S. Yang, and S. Seo: Flexible glucose sensor using CVD-grown graphene-based field effect transistor. *Biosens. Bioelectron.* **37**, 82 (2012).
108. H. Lian, Z. Sun, X. Sun, and B. Liu: Graphene doped molecularly imprinted electrochemical sensor for uric acid. *Anal. Lett.* **45**, 2717 (2012).
109. Y-R. Kim, S. Bong, Y.-J. Kang, Y. Yang, R.K. Mahajan, J.S. Kim, and H. Kim: Electrochemical detection of dopamine in the presence of ascorbic acid using graphene modified electrodes. *Biosens. Bioelectron.* **25**, 2366 (2010).
110. M. Mallesha, R. Manjunatha, C. Nethravathi, G.S. Suresh, M. Rajamathi, J.S. Melo, and T.V. Venkatesha: Functionalized-graphene modified graphite electrode for the selective determination of dopamine in presence of uric acid and ascorbic acid. *Bioelectrochemistry* **81**, 104 (2011).
111. Y. Yu, Z. Chen, B. Zhang, X. Li, and J. Pan: Selective and sensitive determination of uric acid in the presence of ascorbic acid and dopamine by PDDA functionalized graphene/graphite composite electrode. *Talanta* **112**, 31 (2013).
112. Y. Wang, Y. Li, L. Tang, J. Lu, and J. Li: Application of graphene-modified electrode for selective detection of dopamine. *Electrochem. Commun.* **11**, 889 (2009).
113. X. Zhu, Q. Liu, X. Zhu, C. Li, M. Xu, and Y. Liang: Reduction of graphene oxide via ascorbic acid and its application for simultaneous detection of dopamine and ascorbic acid. *Int. J. Electrochem. Sci.* **7**, 5172 (2012).
114. M. Chao, X. Ma, and X. Li: Graphene-modified electrode for the selective determination of uric acid under coexistence of dopamine and ascorbic acid. *Int. J. Electrochem. Sci.* **7**, 2201 (2012).
115. J.W. Heinecke: Oxidative stress: New approaches to diagnosis and prognosis in atherosclerosis. *Am. J. Cardiol.* **91**, 12A (2003).
116. V. Sosa, T. Moline, R. Somoza, R. Paciucci, H. Kondoh, and M.E. Lleonart: Oxidative stress and cancer: An overview. *Ageing Res. Rev.* **12**, 376 (2013).
117. R.K. Sharma, F.F. Pasqualotto, D.R. Nelson, A.J. Thomas, and A. Agarwal: The reactive oxygen species—Total antioxidant capacity score is a new measure of oxidative stress to predict male infertility. *Hum. Reprod.* **14**, 2801 (1999).
118. H. Xu, H. Dai, and G. Chen: Direct electrochemistry and electrocatalysis of hemoglobin protein entrapped in graphene and chitosan composite film. *Talanta* **81**, 334 (2010).
119. Y. Zhou, S. Liu, H-J. Jiang, H. Yang, and H-Y. Chen: Direct electrochemistry and bioelectrocatalysis of microperoxidase-11 immobilized on chitosan–graphene nanocomposite. *Electroanalysis* **22**, 1323 (2010).
120. Q. Lu, X. Dong, L-J. Li, and X. Hu: Direct electrochemistry-based hydrogen peroxide biosensor formed from single-layer graphene nanoplatelet–enzyme composite film. *Talanta* **82**, 1344 (2010).
121. K. Komori, T. Terse-Thakoor, and A. Mulchandani: Bioelectrochemistry of heme peptide at seamless three-dimensional carbon nanotubes/graphene hybrid films for highly sensitive electrochemical biosensing. *ACS Appl. Mater. Interfaces* **7**, 3647 (2015).
122. J. Wei, J. Qiu, L. Li, L. Ren, X. Zhang, J. Chaudhuri, and S. Wang: A reduced graphene oxide based electrochemical biosensor for tyrosine detection. *Nanotechnology* **23**(33), 335707 (2012).
123. F. Valentini, D. Romanazzo, M. Carbone, and G. Palleschi: Modified screen-printed electrodes based on oxidized graphene nanoribbons for the selective electrochemical detection of several molecules. *Electroanalysis* **24**, 872 (2012).
124. Q. Zhang, Y. Qiao, L. Zhang, S. Wu, H. Zhou, J. Xu, and X.-M. Song: Direct electrochemistry and electrocatalysis of horseradish peroxidase immobilized on water soluble sulfonated graphene film via self-assembly. *Electroanalysis* **23**, 900 (2011).
125. R. Manjunatha, G.S. Suresh, J.S. Melo, S.F. D'Souza, and T.V. Venkatesha: An amperometric bienzymatic cholesterol biosensor based on functionalized graphene modified electrode and its electrocatalytic activity towards total cholesterol determination. *Talanta* **99**, 302 (2012).

https://doi.org/10.1557/jmr.2017.175 Published online by Cambridge University Press

126. T. Balamurugan and S. Berchmans: Non-enzymatic detection of bilirubin based on a graphene–polystyrene sulfonate composite. *RSC Adv.* **5**, 50470 (2015).
127. Y-L. Wang and G-C. Zhao: Electrochemical sensing of nitric oxide on electrochemically reduced graphene-modified electrode. *Int. J. Electrochem.* **2011**, 482780 (2011).
128. D.D. Tu, Y. He, Y.Z. Rong, Y. Wang, and G. Li: Disposable L-lactate biosensor based on a screen-printed carbon electrode enhanced by graphene. *Meas. Sci. Technol.* **27**, 045108 (2016).
129. K. Vijayaraj, S.W. Hong, S.H. Jin, S.C. Chang, and D.S. Park: Fabrication of a novel disposable glucose biosensor using an electrochemically reduced graphene oxide–glucose oxidase biocomposite. *Anal. Methods* **8**, 6974 (2016).
130. F. Liu, K.S. Choi, T.J. Park, S.Y. Lee, and T.S. Seo: Graphene-based electrochemical biosensor for pathogenic virus detection. *BioChip J.* **5**, 123 (2011).
131. F. Liu, Y.H. Kim, D.S. Cheon, and T.S. Seo: Micropatterned reduced graphene oxide based field-effect transistor for real-time virus detection. *Sens. Actuators, B* **186**, 252 (2013).
132. Q. Wang, J. Su, J. Xu, Y. Xiang, R. Yuan, and Y. Chai: Dual amplified, sensitive electrochemical detection of pathogenic sequences based on biobarcode labels and functional graphene modified electrode. *Sens. Actuators, B* **163**, 267 (2012).
133. M.S. Mannoor, H. Tao, J.D. Clayton, A. Sengupta, D.L. Kaplan, R.R. Naik, N. Verma, F.G. Omenetto, and M.C. McAlpine: Graphene-based wireless bacteria detection on tooth enamel. *Nat. Commun.* **3**, 763 (2012).
134. C-Y. Chan, J. Guo, C. Sun, M.-K. Tsang, F. Tian, J. Hao, S. Chen, and M. Yang: A reduced graphene oxide-Au based electrochemical biosensor for ultrasensitive detection of enzymatic activity of botulinum neurotoxin A. *Sens. Actuators, B* **220**, 131 (2015).
135. Y. Wan, Z. Lin, D. Zhang, Y. Wang, and B. Hou: Impedimetric immunosensor doped with reduced graphene sheets fabricated by controllable electrodeposition for the non-labelled detection of bacteria. *Biosens. Bioelectron.* **26**, 1959 (2011).
136. L.C. Xiang, Z. Wang, Z.H. Liu, S.N.E. Weigum, Q.K. Yu, and M.Y. Chen: Inkjet-printed flexible biosensor based on graphene field effect transistor. *IEEE Sens. J.* **16**, 8359 (2016).
137. S. Karapetis, G.P. Nikoleli, C.G. Siontorou, D.P. Nikolelis, N. Tzamtzis, and N. Psaroudakis: Development of an electrochemical biosensor for the rapid detection of cholera toxin based on air stable lipid films with incorporated ganglioside GM1 using graphene electrodes. *Electroanalysis* **28**, 1584 (2016).
138. J. Basu and C. RoyChaudhuri: Attomolar sensitivity of FET biosensor based on smooth and reliable graphene nanogrids. *IEEE Electron Device Lett.* **37**, 492 (2016).

https://doi.org/10.1557/jmr.2017.175 Published online by Cambridge University Press